SLAC-PUB-1777
July 1976

HIGH-$p_\perp$ DYNAMICS*

J. D. Bjorken
Stanford Linear Accelerator Center
Stanford University, Stanford, California 94305

These lectures do not attempt to review this subject, but only to look at a rather restricted, but topical, portion. My main reason (or excuse) for such a limitation is the existence of an excellent, up-to-date, comprehensive review by Sivers, Brodsky, and Blankenbecler (SBB).[1] In addition, very recent results on high-$p_\perp$ correlation measurements from the ISR at CERN and reported at the Palermo Conference have, I believe, a large impact on the theoretical interpretations.

Therefore, these lectures will lean heavily on the new ISR data. However, rather than recite a long set of experimental results, I shall take even more liberties and use the data somewhat selectively to illuminate the status of my own favorite theoretical interpretation—the hard collision model.

I will not apologize for such outrageous bias, but only acknowledge it, because I feel that the new evidence, while far from conclusive, tilts strongly in favor of hard-collision ideas.

In the following, we shall first formulate the hard-collision model in terms of three general hypotheses about the phase-space populations of produced particles in high-$p_\perp$ events, illustrating their experimental status with ISR data.

---

* Work supported by the Energy Research and Development Administration.
(Extracted from the Proceedings of Summer Institute on Particle Physics, SLAC Report No. 191, November 1975)

Then we shall illustrate the hard-collision mechanism by examining the theory of pp-collisions which include exchange of a high-$p_\perp$ photon. This has a clear connection with deep-inelastic electroproduction processes, themselves hard-collision reactions. Study of such prototype hard collisions provides a way of estimating the properties of the observed collisions (which, however, are apparently of strong, not electromagnetic, origin). Finally, we discuss more specific models of the binary hard-collisions, in particular the constituent interchange model—by far the most successful attempt to organize and interpret the data.

I. EXPERIMENTS, REFERENCES, AND A CAPSULE SUMMARY OF THE PHENOMENON

The first experiment on the high-$p_\perp$ phenomenon was that of the CERN-Columbia-Rockefeller Group (CCR) at the CERN Intersecting Storage Rings (ISR), which measured inclusive π^0 production out to $p_\perp \sim 9$ GeV. This and subsequent inclusive spectrum experiments are reviewed in SBB. Recent ISR experiments to which we shall refer include the following:

(i) CCRS (CERN-Columbia-Rockefeller-Saclay): A double arm charged particle spectrometer triggered by a high-$p_\perp$ π^0 incident on lead glass at the back of one spectrometer arm. $P/K/\pi$ separation only exists below 1 GeV (using time-of-flight techniques).

(ii) ACHM (Aachen-CERN-Heidelberg-Munich): A streamer chamber (nearly 4π solid angle acceptance) triggered by a π^0 into lead glass. Multiplicity and rapidity of charged secondaries are observed, but momenta are not measured.

(iii) CERN-SFM: Charged particle momenta measured in the split-field magnet (SFM) facility (nearly 4π angular acceptance). The trigger is again lead glass at 90°.

(iv) DLR (Daresbury-Liverpool-Rutherford): Single-arm spectrometer (with

P/K/π identification) with a "barrel" of scintillation counters ($\sim 4\pi$ solid angle acceptance) to count associated charged particles.

(v) CCHK (CERN-College de France-Heidelberg-Karlsruhe): Again the split-field magnet, but with a forward, positive high-$p_\perp$ particle as the trigger. Their data appears to be at somewhat lower $p_\perp$, and I will not discuss it here.

I list here the primary references I have used:

P. Darriulat, summary report at the Palermo Conference, which will appear in the Proceedings.

ACHM

K. Eggert, K. L. Giboni, W. Thomé, B. Betev, P. Darriulat, P. Dittman, M. Holder, K. McDonald, T. Modis, H. Pugh, G. Vesztergombi, V. Eckhardt, H. Gebauer, R. Meinke, O. Sander, and P. Seyboth,

"A Study of High Transverse Momentum π^0's at ISR Energies" (submitted to Palermo Conference)

"Angular Correlations among Charged Particles Observed in Association with a High Transverse Momentum π^0 at the CERN-ISR"(submitted to Palermo Conference)

CERN-SFM

P. Darriulat, P. Dittman, K. Eggert, M. Holder, K. McDonald, T. Modis, F. Navarria, A. Seiden, J. Strauss, G. Vesztergombi, and E. Williams,

"An Inclusive Measurement of Charged Particles Accompanying a High Transverse Momentum π^0 at the ISR Split-Field Magnet Facility" (submitted to Palermo Conference)

CCRS

F. Büsser, L. Camilleri, L. DiLella, B. Pope, B. Blumenfeld, S. White, A. Rothenberg, S. Segler, M. Tannenbaum, M. Banner, J. Chèze, J. Hamel,

H. Kasha, J. Pansart, G. Smadja, J. Teiger, H. Zaccone, and A. Zylberstejn,

"High Transverse Momentum Phenomena Involving π^0 and η Mesons at the CERN ISR" (submitted to Palermo Conference).

A most important reference is

D. Sivers, S. Brodsky, and R. Blankenbecler

"High Transverse Momentum Phenomena," SLAC-PUB-1595 (to be published in Physics Reports).

Much of these lectures follow, for better or worse, my own review two years ago at the Aix-en-Provence Conference: Journal de Physique, Suppl. 10, 34, 385 (1973).

We conclude this introduction by briefly reminding the reader of the main features of high-$p_\perp$ physics at FNAL and ISR energies:

(1) The inclusive π^0 spectrum at high $p_\perp$ falls more slowly than an exponential in $p_\perp$. Recent data from ACHM is shown in Fig. 1 and from CCRS in Fig. 2.

(2) At fixed large $p_\perp$ the spectrum rises sharply with $\sqrt{s}$.

(3) The fraction of heavy particles (K, $\bar{K}$, p, $\bar{p}$) increases at high $p_\perp$, typically being $\sim$ 30% for $p_\perp > 2$ GeV. At FNAL, $K^+/\pi^+ \sim 1/2$ and stable, while $\bar{p}/p$ and K^-/K^+ are small but increasing with $\sqrt{s}$. At the ISR, $p \approx \bar{p}$ and $K^+ \sim K^-$ for $p_\perp \sim 2 - 3$ GeV. At larger $p_\perp$, $\bar{p}/p$ and K^-/K^+ again begin to decrease.

II. GENERAL DEFINITION OF THE HARD COLLISION MODEL

The simplest and most natural way of defining the hard collision model is in terms of specific models (multiperipheral, bremsstrahlung, parton, etc.) which in some manner reduce the origin of the high-$p_\perp$ systems to a binary collision of the projectiles or some sub-units thereof. Such models are epitomized by the diagram in Fig. 3, where the star indicates the only element containing exchange

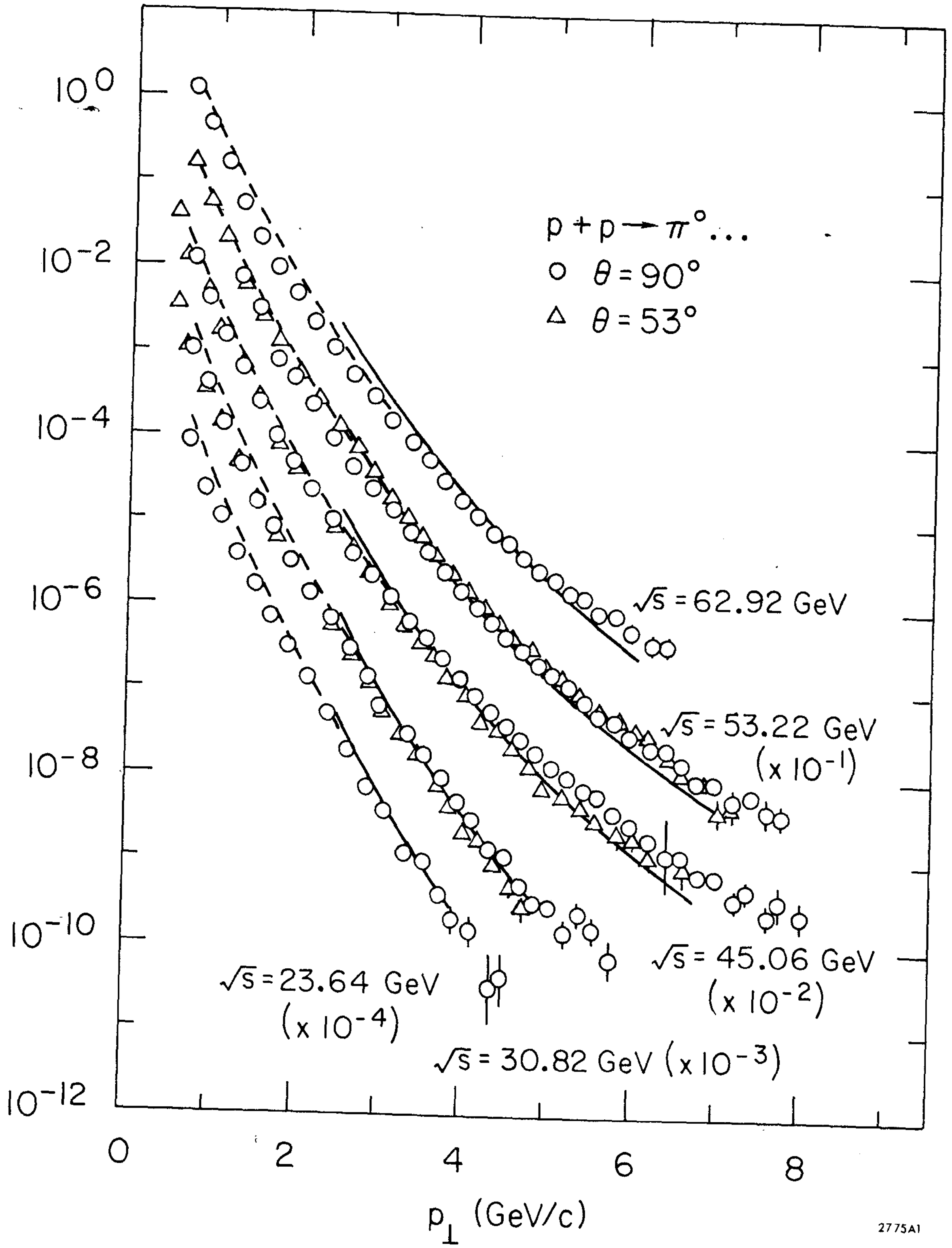

Fig. 1. Inclusive π^{0} spectrum $E\,\frac{d\sigma}{d^3p}$ for $\theta_{cm} = 90^{0}$. Data are from ACHM.

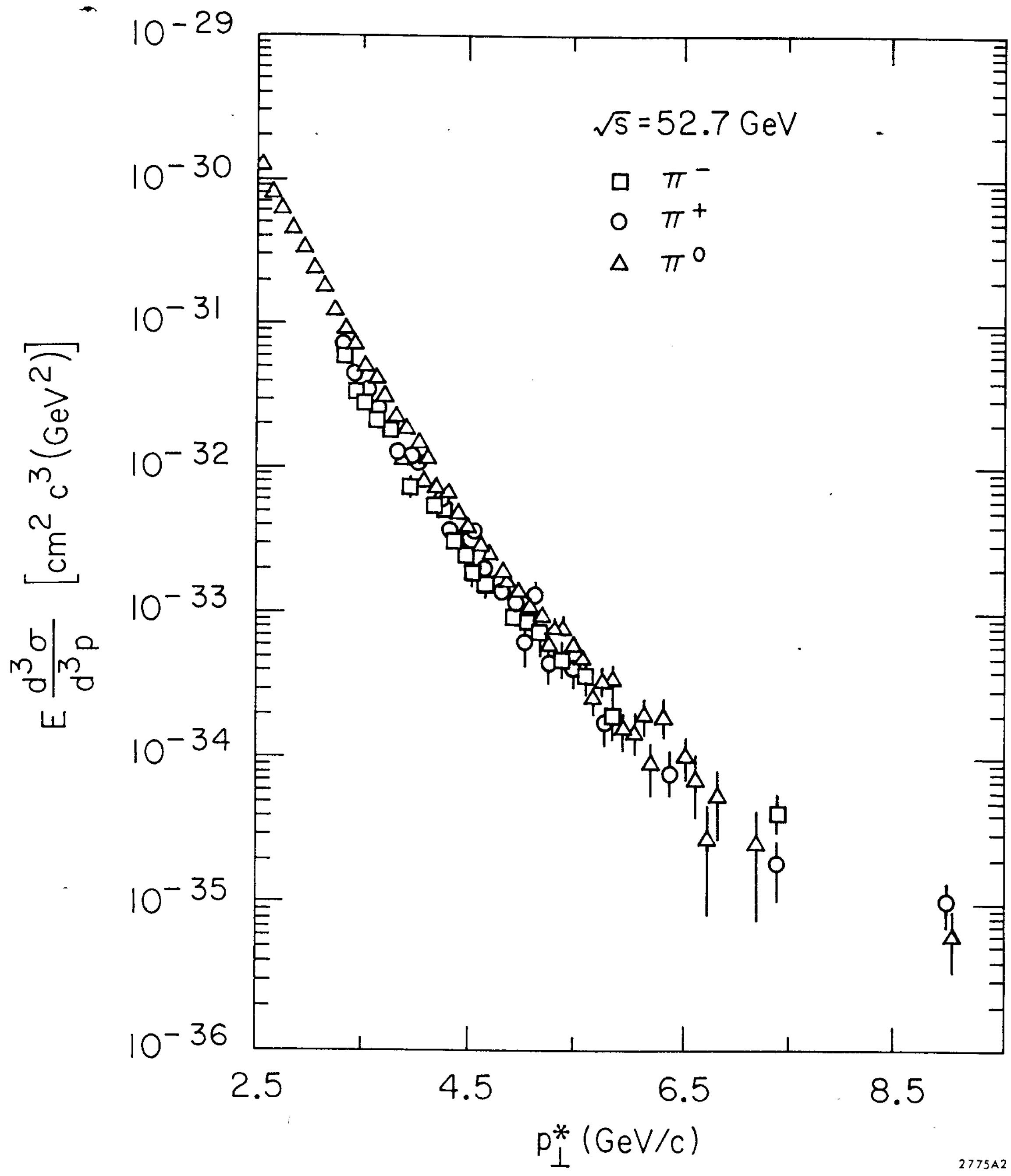

Fig. 2. Charged and neutral particle spectra for $\theta_{cm} = 90^{\circ}$. Data are from CCRS.

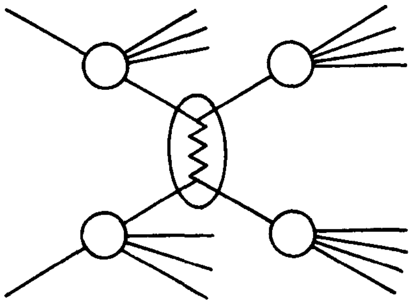

2775A3

Fig. 3. Typical diagram exhibiting the hard collision mechanism.

of large $p_\perp$. However, there is a more general definition, which has the advantage of being an operational definition, and which includes all such models as special cases. This generalization may be phrased in terms of 3 hypotheses concerning the phase-space populations of particles in high-$p_\perp$ events. The first is

Hypothesis A: Coplanarity

Define a plane by the beam directions (in a collinear frame of reference) and by the direction of the highest-$p_\perp$ particle in the event. Then consider the other produced particles and let p_N be the component of momentum normal to the plane so defined. Then the coplanarity hypothesis is that dN/dp_N should fall steeply with increasing p_N. Perhaps

$$\frac{dN}{dp_N} \sim e^{-bp_N} = e^{-\frac{p_N}{\langle p_N \rangle}} \tag{2.1}$$

where $\langle p_N \rangle$ is small, much less than 1 GeV.

The evidence concerning this hypothesis comes from CCR and CERN-SFM, and is somewhat contradictory. For events with two opposite-side high-$p_\perp$ π^o's with $p_\perp > 2$ GeV, CCR finds[2]

$$\langle p_N \rangle \sim 1.3 \pm 0.2 \text{ GeV} \tag{2.2}$$

very large indeed. However, CERN-SFM has measured (cf Fig. 4) opposite-side charged particles produced in association with a π^o trigger with $\langle p_\perp \rangle \sim 2.4$ GeV and find

$$\langle p_N \rangle \sim 0.5 - 0.6 \text{ GeV} \tag{2.3}$$

We shall return to this question later when we consider prototype hard collisions, in order to estimate what $\langle p_N \rangle$ ought to be.

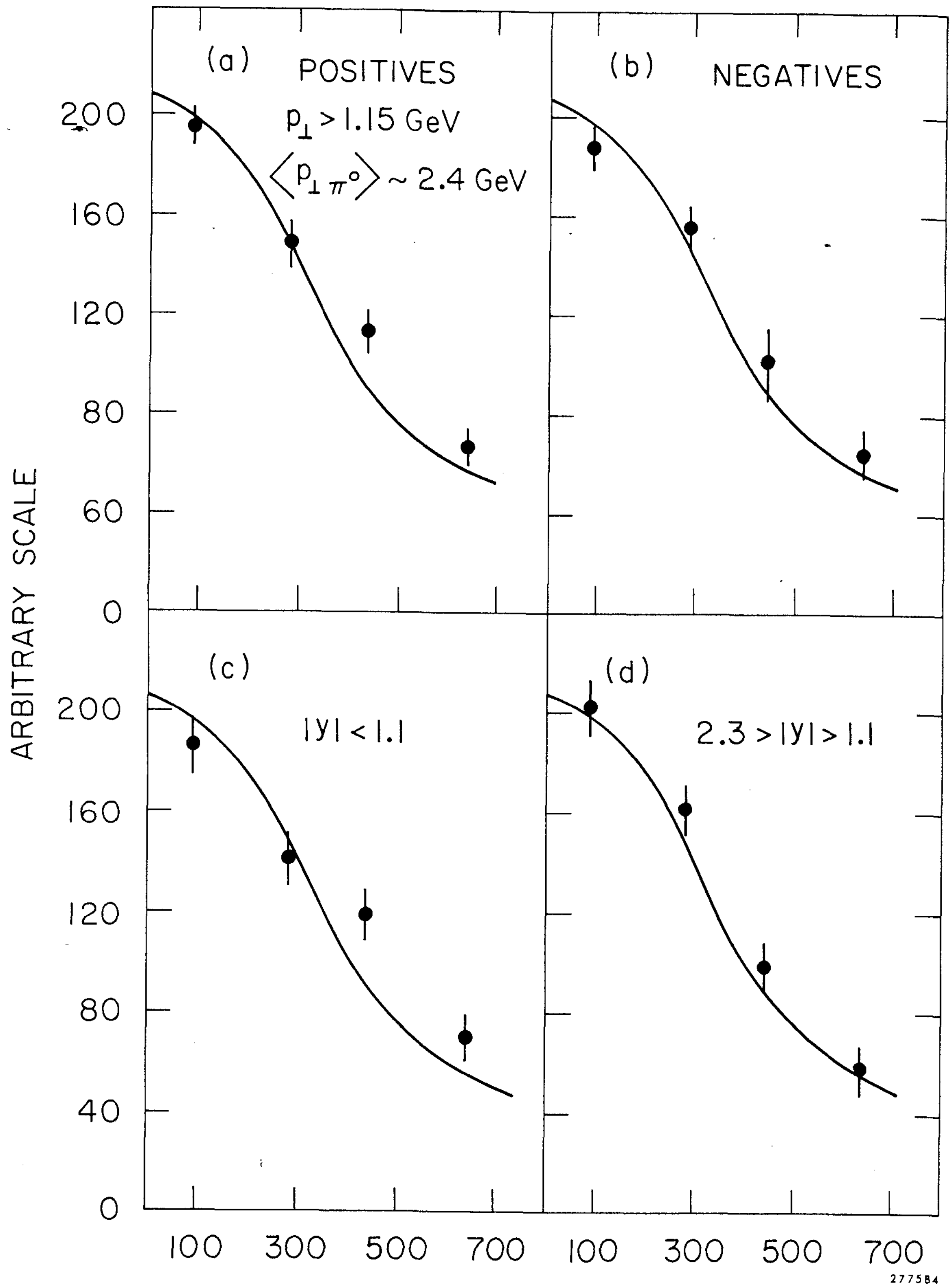

Fig. 4. Distribution in p_N of opposite-side charged particles produced in association with a π^0 trigger with $\langle p_\perp \rangle \sim 2.4$ GeV. Data are from CERN-SFM.

Hypothesis B: Jet on the Same Side

Any other high-$p_\perp$ particles emitted in the same hemisphere as the highest-$p_\perp$ particle emerge in the same direction. That is:

(i) The mass distribution of such pairs is bounded and increases only slowly as the transverse momenta $p_{1\perp}$ and $p_{2\perp}$ increase.

(ii) The rapidity distribution $\frac{dN}{dy_2}$ of the second particle peaks at y_1 and the peaking sharpens as p_2 increases.

(iii) If $y_2 \ll y_1$ or $y_2 \gg y_1$, the same-side 2-particle correlation function is small.

Empirically, as found by CCR, two-particle same-side correlation functions are large ($\sim 10^{2\pm1}$) when the $p_\perp$ of both particles are large, and $y_1 \sim y_2$. Some recent data from CCRS (Fig. 5) show this effect. They observe an inclusive spectrum of charged particles which decreases slowly with increasing momentum provided a high-$p_\perp$ π^0 (in the same direction as the charged particle) is required in the event.

Given the existence of such a positive correlation, we should, according to this hypothesis, see the correlation diminish rapidly as Δy of the two particles increases. Such an effect is seen by ACHM (Fig. 6, 7), who observe the rapidity distribution of charged particles accompanying a high-$p_\perp$ π^0. There is an excess same-side component which peaks at the rapidity of the π^0. CERN-SFM also measures the distribution of high-$p_\perp$ same-side dipions (one charged, one neutral). Figure 8 again shows that the rapidity distribution of high-$p_\perp$ charged hadrons peaks at the rapidity of the associated π^0, and that, as expected, the peaking sharpens as $p_\perp$ increases. This is corroborated by the measured mass-distribution of the dipion system, which is peaked below 1 GeV, independent of $p_\perp$.

Thus the evidence for Hypothesis B seems to be quite strong.

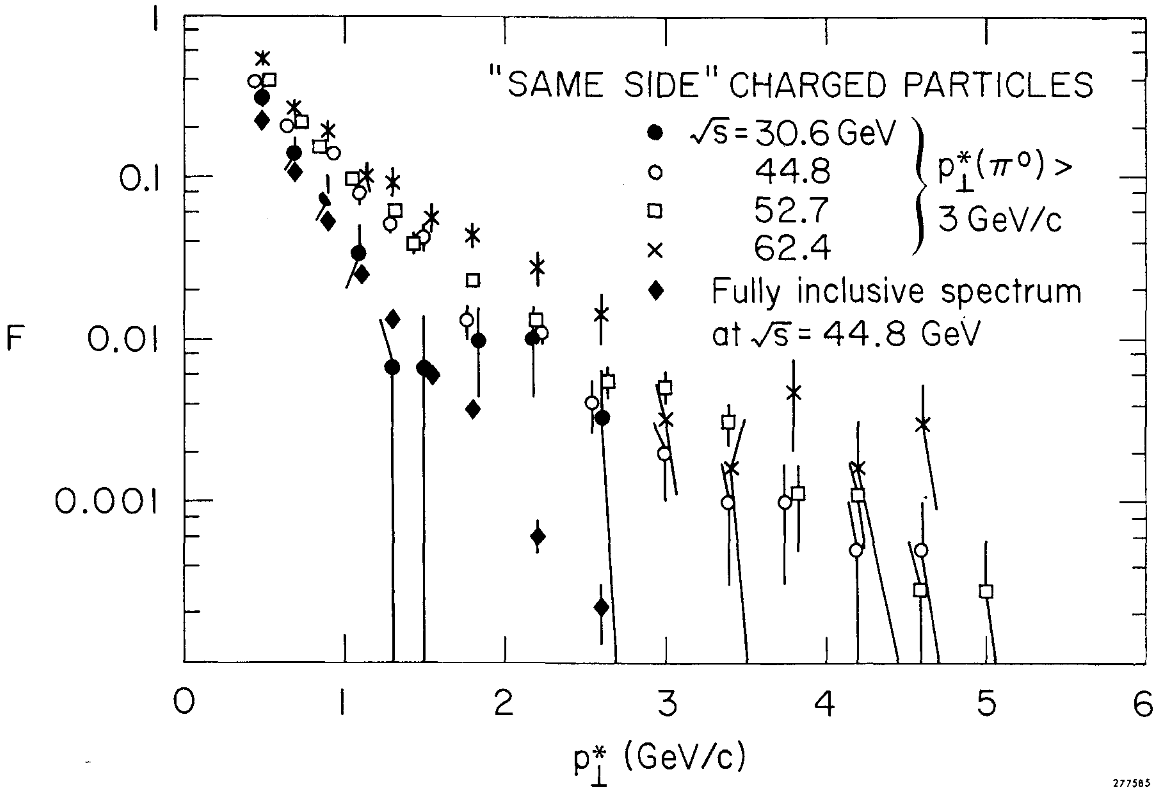

Fig. 5. Invariant cross section for charged particles produced alongside a π^0 trigger of momentum 3 GeV. The data are from CCRS.

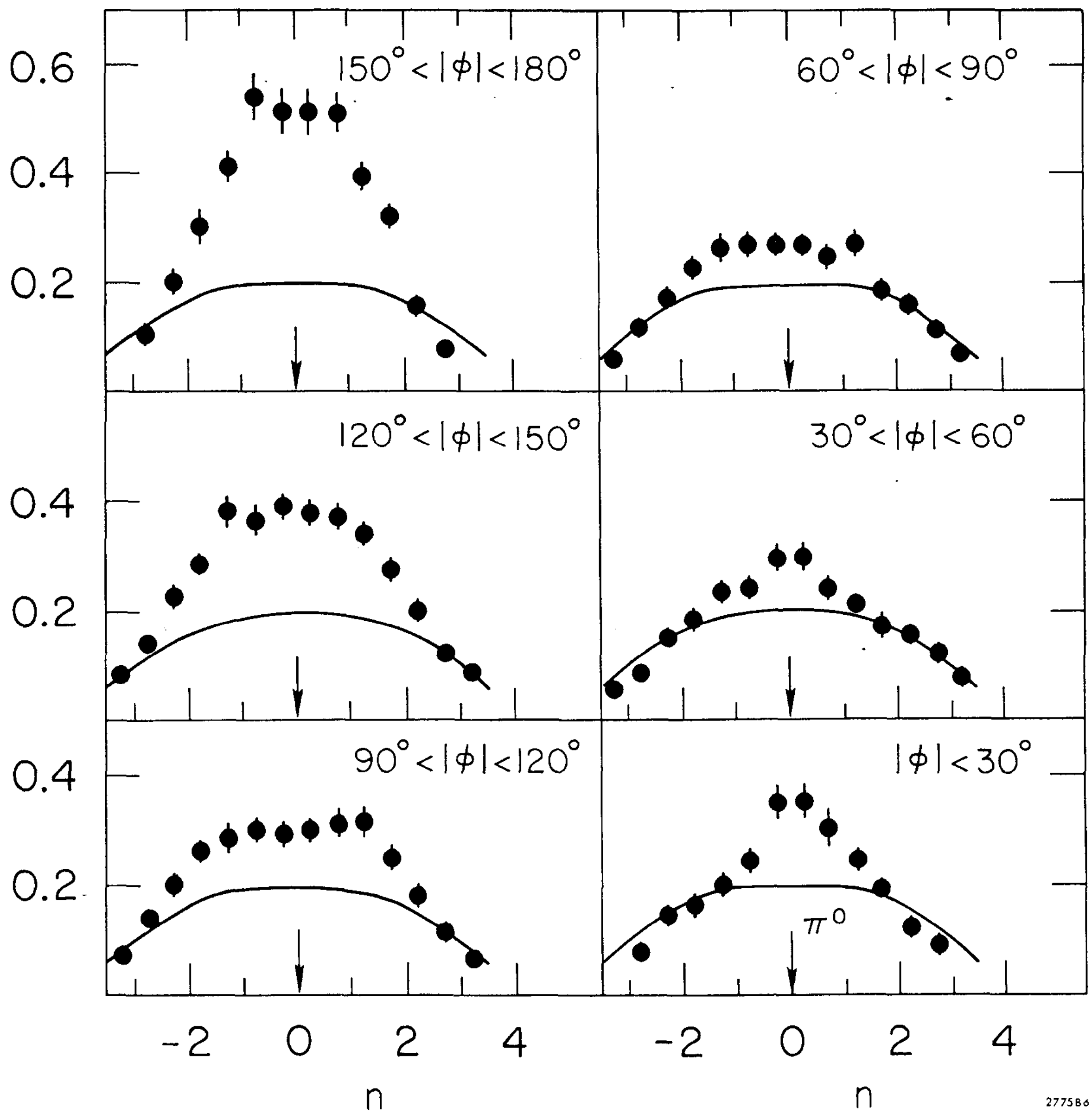

Fig. 6. Charged particle densities in interactions where a π^0 with $p_\perp > 2$ GeV is produced at 90°. The data are from ACHM at $\sqrt{s} = 53$ GeV. The lines indicate densities in interactions without large-$p_\perp$ production.

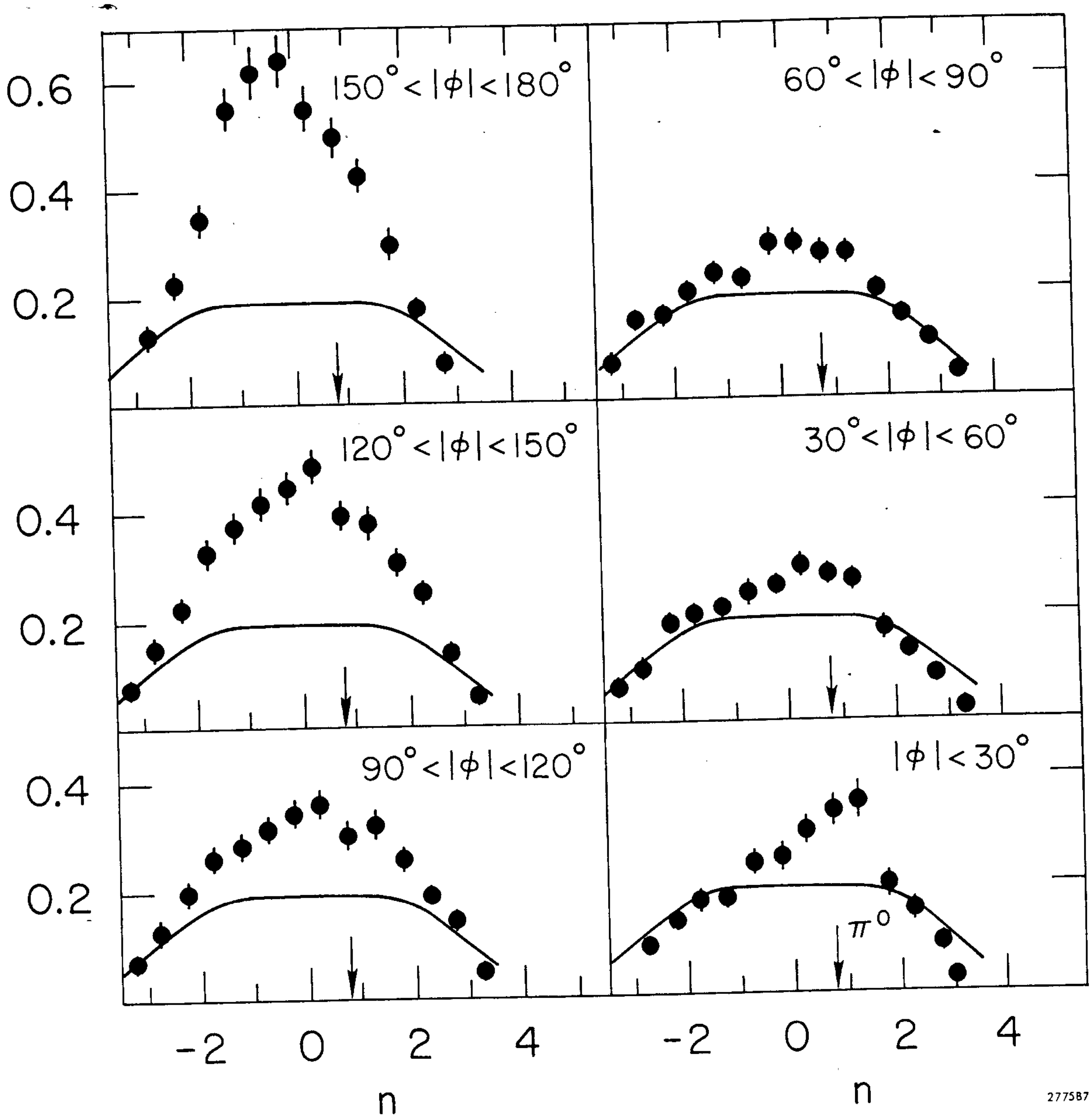

Fig. 7. Same as Fig. 6, except that the trigger π^0 is at $\theta = 53^\circ$, and 3 GeV < $p_\perp$ < 5 GeV.

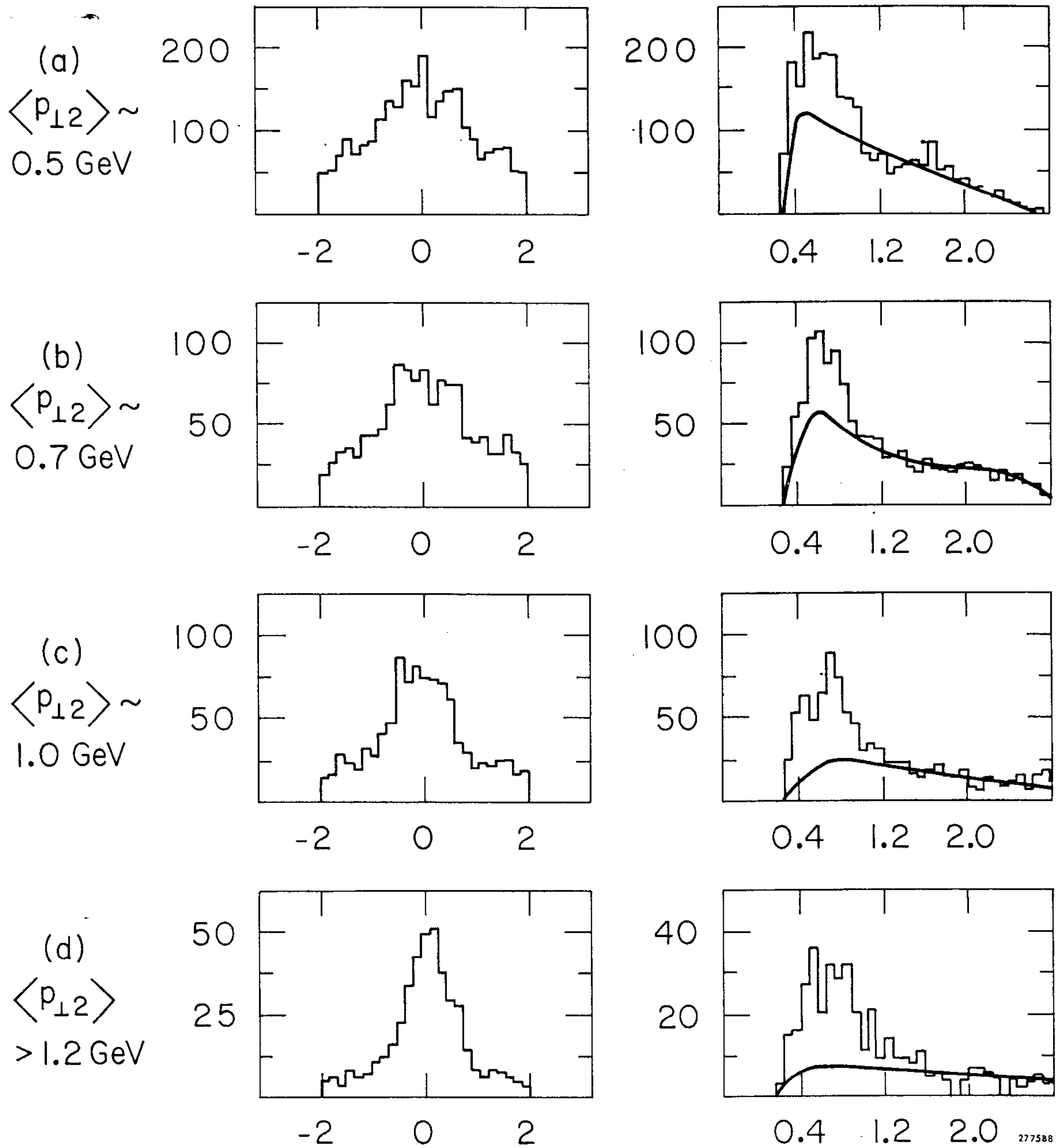

Fig. 8. Rapidity and mass-distributions of charged particles produced in association with a trigger π^0 at 90^0 with $p_\perp \sim 2$ GeV: (a) $\langle p_{\perp\, ch} \rangle \sim 0.5$ GeV; (b) $\langle p_{\perp\, ch} \rangle$ · 0.7 GeV; (c) $\langle p_{\perp\, ch} \rangle \sim 1.0$ GeV; (d) $\langle p_{\perp\, ch} \rangle > 1.2$ GeV. Data are from CERN-SFM.

Hypothesis C: Jet on the Opposite Side

This hypothesis comes in two parts. The first part is that there exists at least one high-$p_\perp$ particle on the side opposite the highest $p_\perp$ particle in the event. The only way to avoid this would be to have an excess opposite-side multiplicity $\Delta\bar{n}$ large and growing linearly with $p_\perp$. However, the data shows a considerably smaller amount; ACHM quotes an opposite-side excess multiplicity $\Delta n_{ch} = 3.7 \pm 0.3$ at a $p_\perp$ for the trigger π^0 of 5 GeV. Even after allowance for neutrals, this amounts to a $p_\perp$ of ~ 1 GeV per excess particle. Figures 9 - 11 show some of the evidence for this multiplicity increase. The DLR data show that it is approximately independent of the nature of the trigger particle. There is further evidence with a similar conclusion from CCRS, to which we shall return later.

The main part of Hypothesis C is that all other high-$p_\perp$ particles emerge in the same direction as the highest-p opposite-side particle (i.e., Hypothesis B repeated again). As yet, there is no data in support of this hypothesis, but there would seem to be no reason why CERN-SFM should not be able to soon supply it.

A frequent point of confusion lies in the breadth Δy of the opposite side rapidity distribution of the excess "balancing" particles. Experimentally $\Delta y \sim 4$, very large. This, however, does not measure the width of the rapidity distribution of the components of the opposite-side jet (which should be small, $\Delta y < 2$), but the distribution in rapidity of the jet axes themselves, averaged over many events. This is expected to be broad. The breadth of the opposite-side rapidity distribution has been measured (Fig. 12) by CERN-SFM as a function of the $p_\perp$ of the opposite-side particle. It is roughly independent of $p_\perp$, with $\Delta y \sim 4$ (FWHM).

We may conclude that there is general consistency of the data with the three hard-collision hypotheses A, B, and C, although the older CCR data is inconsistent with A, and C is not fully tested experimentally.

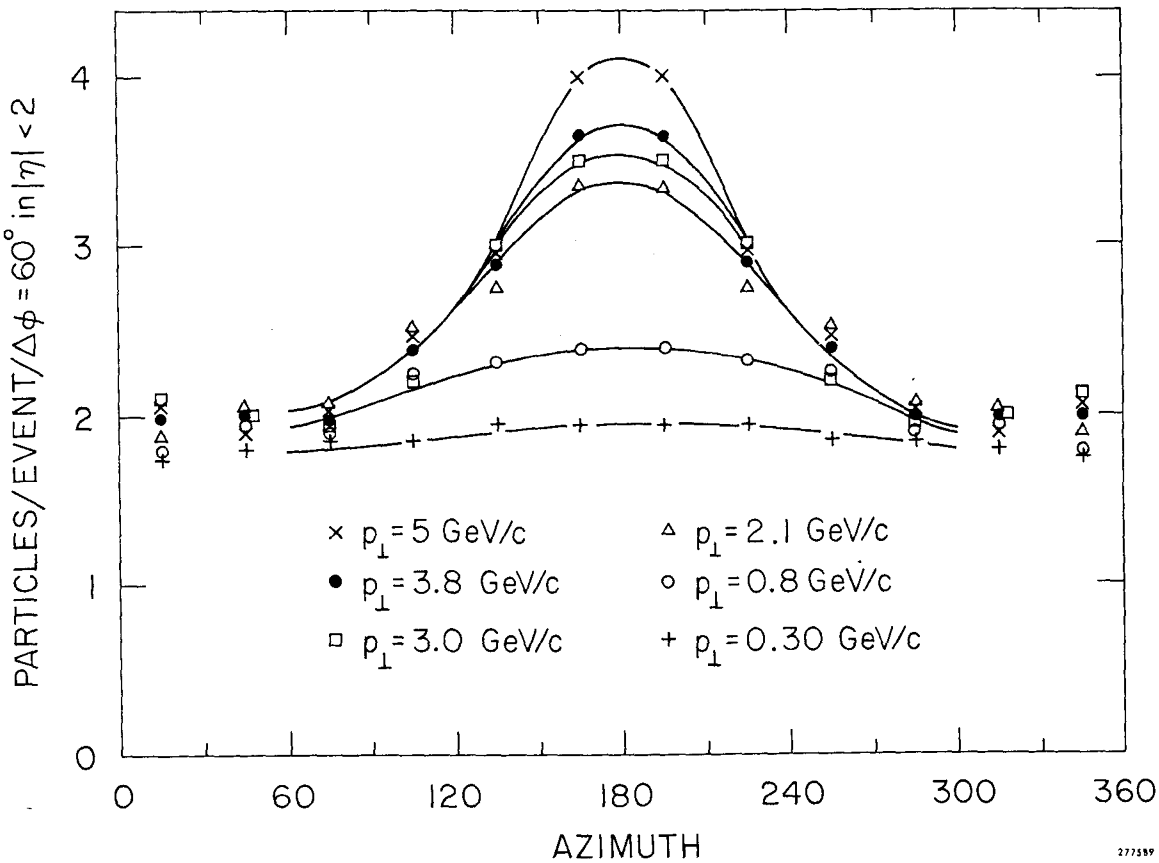

Fig. 9. Charged-particle density in a rapidity range -2 to +2 associated with a trigger π^0 at $\theta = 90^0$, $\phi = 0$ and various $p_\perp$. Data are from ACHM.

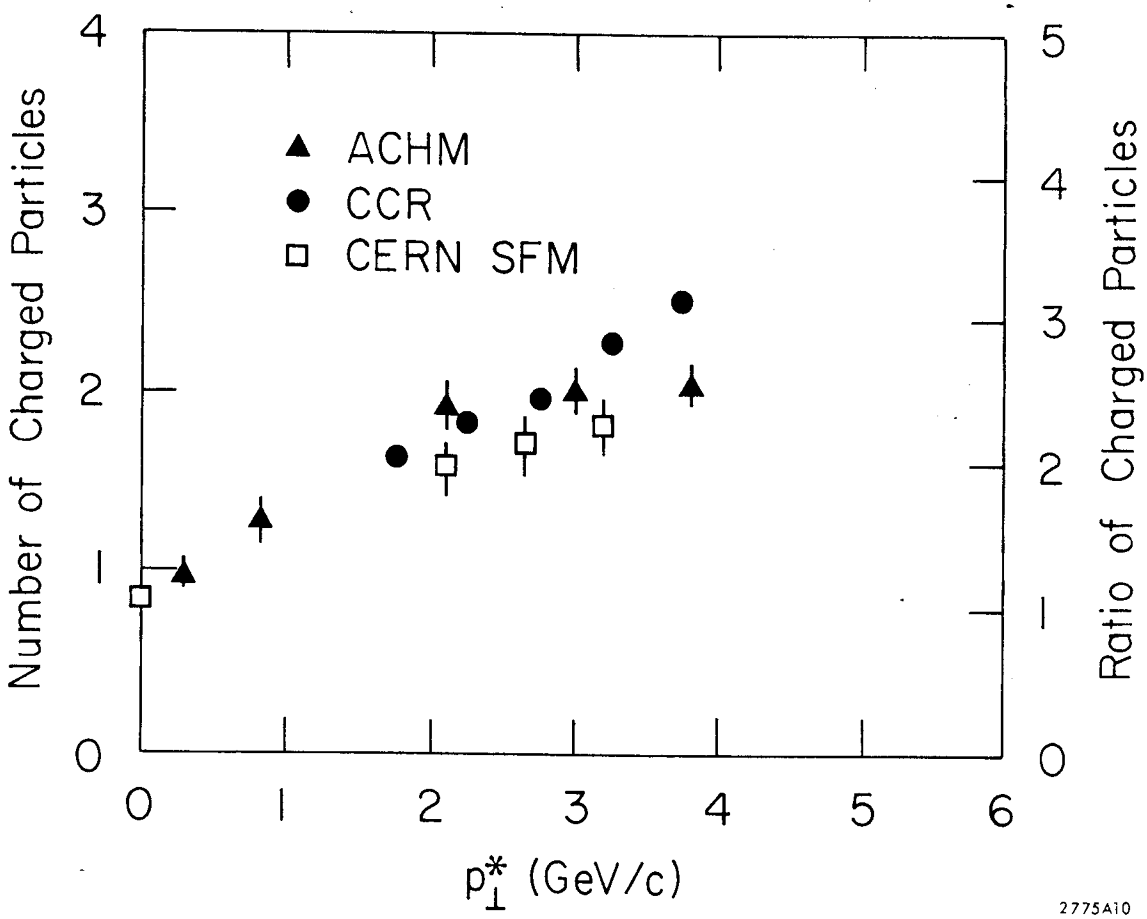

Fig. 10. Increase of charged particle density in a region $\Delta\phi = \pm 30^o$ and $\Delta y = \pm 1$ opposite to a 90^o π^o trigger.

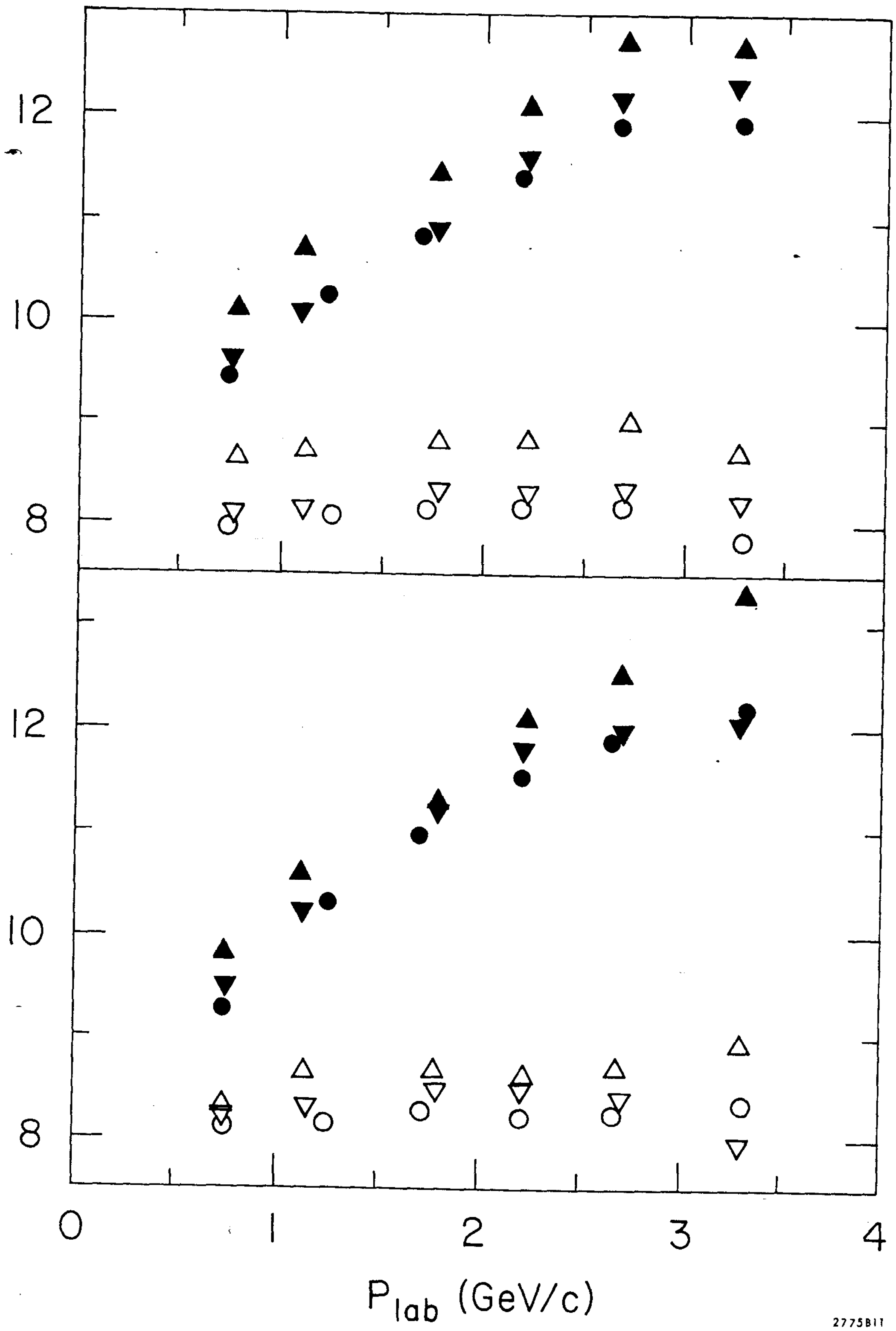

Fig. 11. Opposite-side multiplicities (in a limited solid angle) toward (open symbols) or away from a 90^{o} charged hadron of momentum $p_{\perp}$. The hadron is identified as a π (●), K (▼) or p (▲) with positive charge (upper figure) or negative charge (lower figure). Data are from DLR (preliminary).

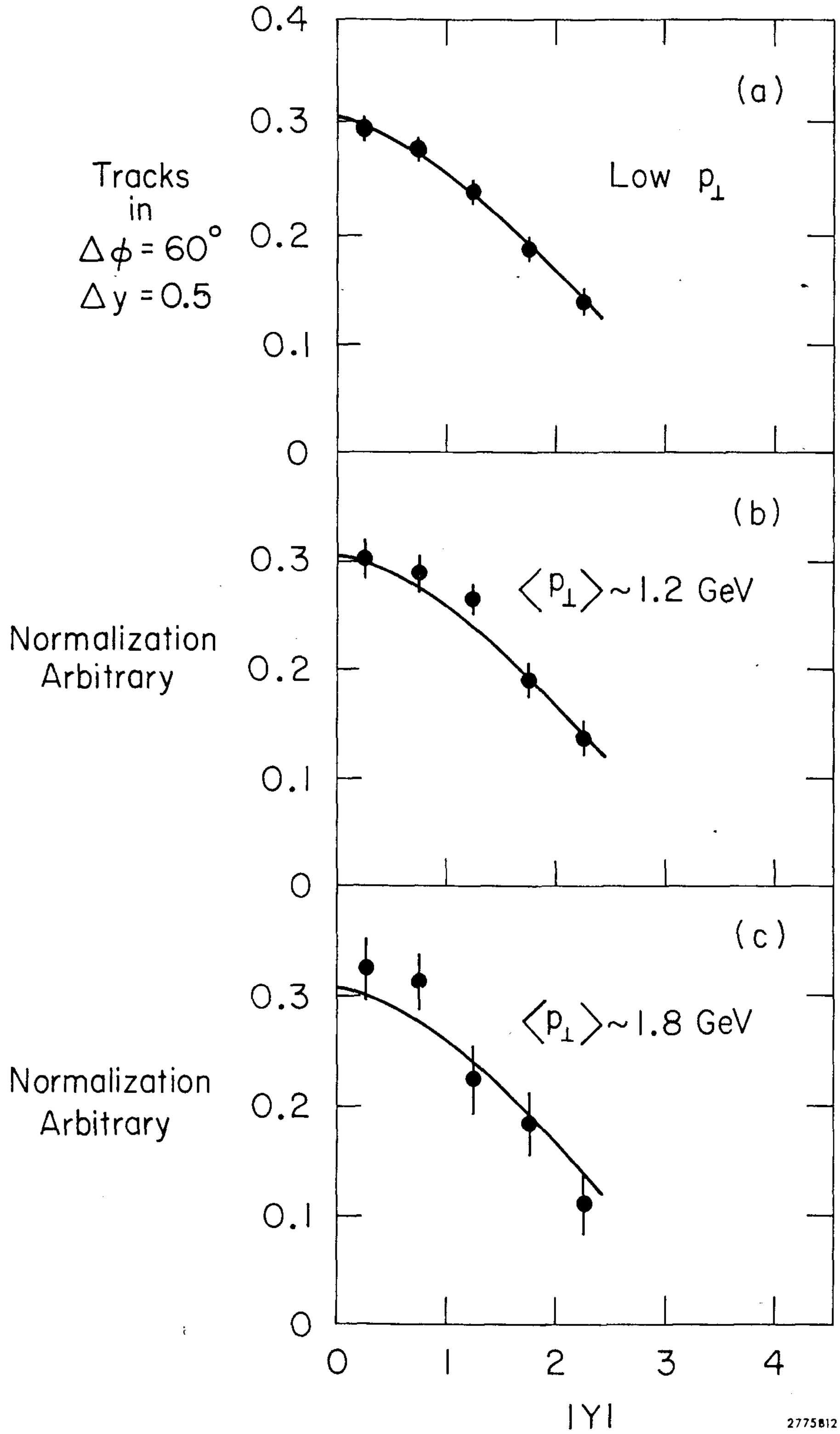

Fig. 12. Rapidity distributions of charged particles produced within $\pm 30^\circ$ of azimuth opposite to a π^0 of $\theta = 90^\circ$ and $p_\perp \lesssim 2$ GeV: (a) low $p_\perp$; (b) $\langle p_\perp \rangle \sim 1.2$ GeV; (c) $\langle p_\perp \rangle \sim 1.8$ GeV. Data are from CERN-SFM.

Before continuing with a more quantitative discussion of the evidence, we conclude this section with some further data on correlations:

(i) Data from CCRS show that the distribution of opposite-side charged particles (at $\theta_{cms} = 90^0$) does not depend upon $\sqrt{s}$ (Fig. 13). It exhibits again a large value for the 2-particle correlation function, comparable to that found at high energy on the same side.

(ii) The low-$p_\perp$ component of the associated particles seems not to be strongly correlated with the existence of a high-$p_\perp$ particle. Such data comes mainly from ACHM, and their papers should be consulted for the detailed evidence. An example is given in Fig. 14.

III. EXAMPLES OF THE HARD COLLISION MECHANISM

A simple prototype of a hard collision is deep inelastic electron-proton scattering. In the laboratory frame, one naturally considers it as a collision of a virtual photon and the proton. The populations of produced particles will peak at low $p_\perp$ and be distributed over all rapidities, with photon-fragmentation region[3] (length $\sim$ log Q^2 in rapidity space) and proton fragmentation region (length $\sim$ 2) at the extremes. This is illustrated in Fig. 15b. In the e-p center-of-mass frame, this same population maps into that of Fig. 15c. Half the photon fragmentation region maps into a high-$p_\perp$ "jet," and the electron (plus soft bremsstrahlung) is found on the opposite side, balancing the $p_\perp$. The remainder of the produced hadrons (as well as bremsstrahlung photons) goes down the beam direction. Thus the structure of the event is that of three "jets" (with a fourth consisting of soft bremsstrahlung radiated by the incident electron). The process satisfies all the hard-collision hypotheses, provided the mean $\langle p_\perp \rangle$ of virtual photon fragments (as seen in the laboratory frame) remains small, even for large Q^2. The evidence regarding this will be reviewed in the next section.

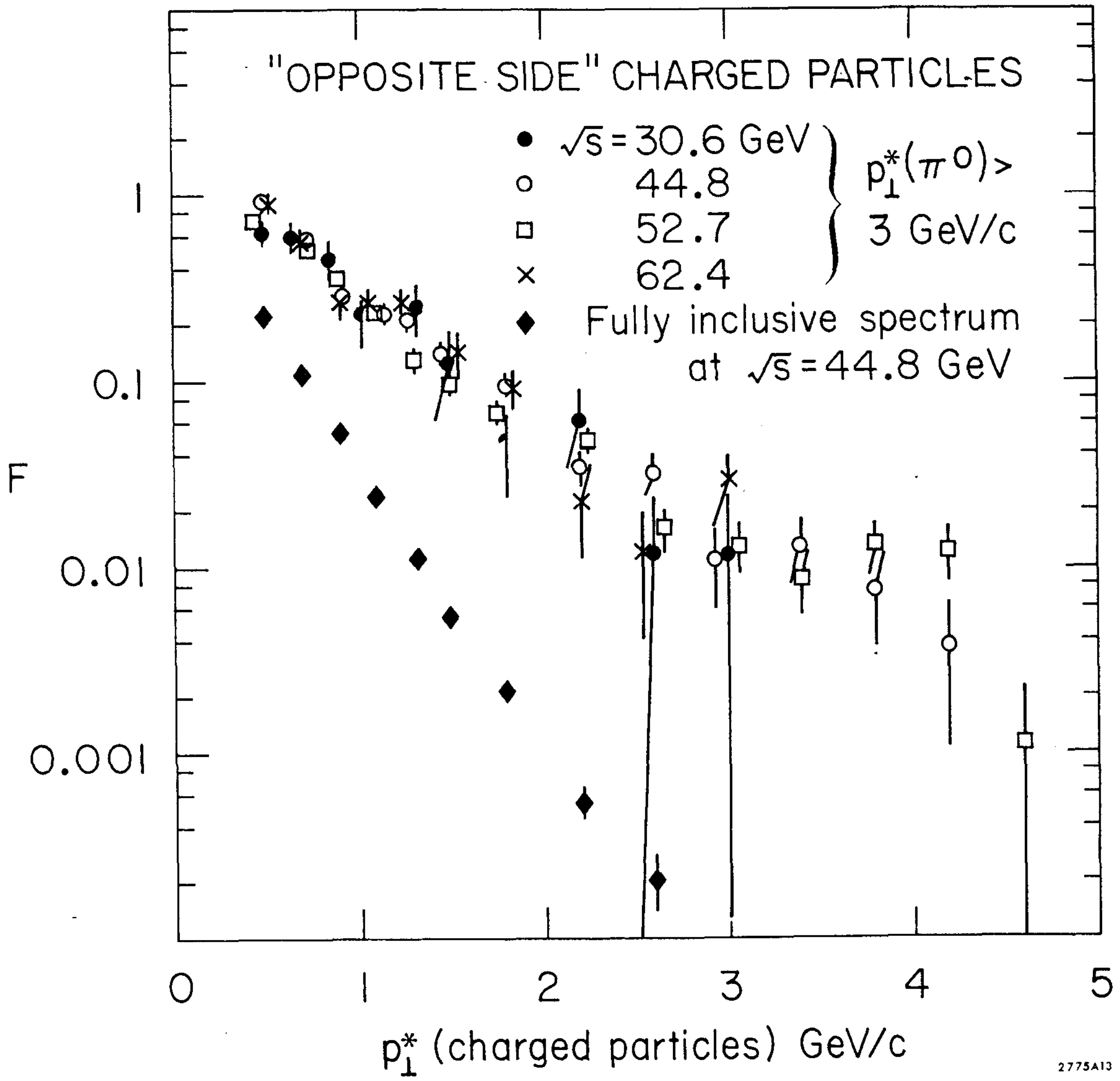

Fig. 13. Invariant cross section for charged particles produced in association with an opposite-side π^0 with $p_\perp$ > 3 GeV. Data are from CCRS.

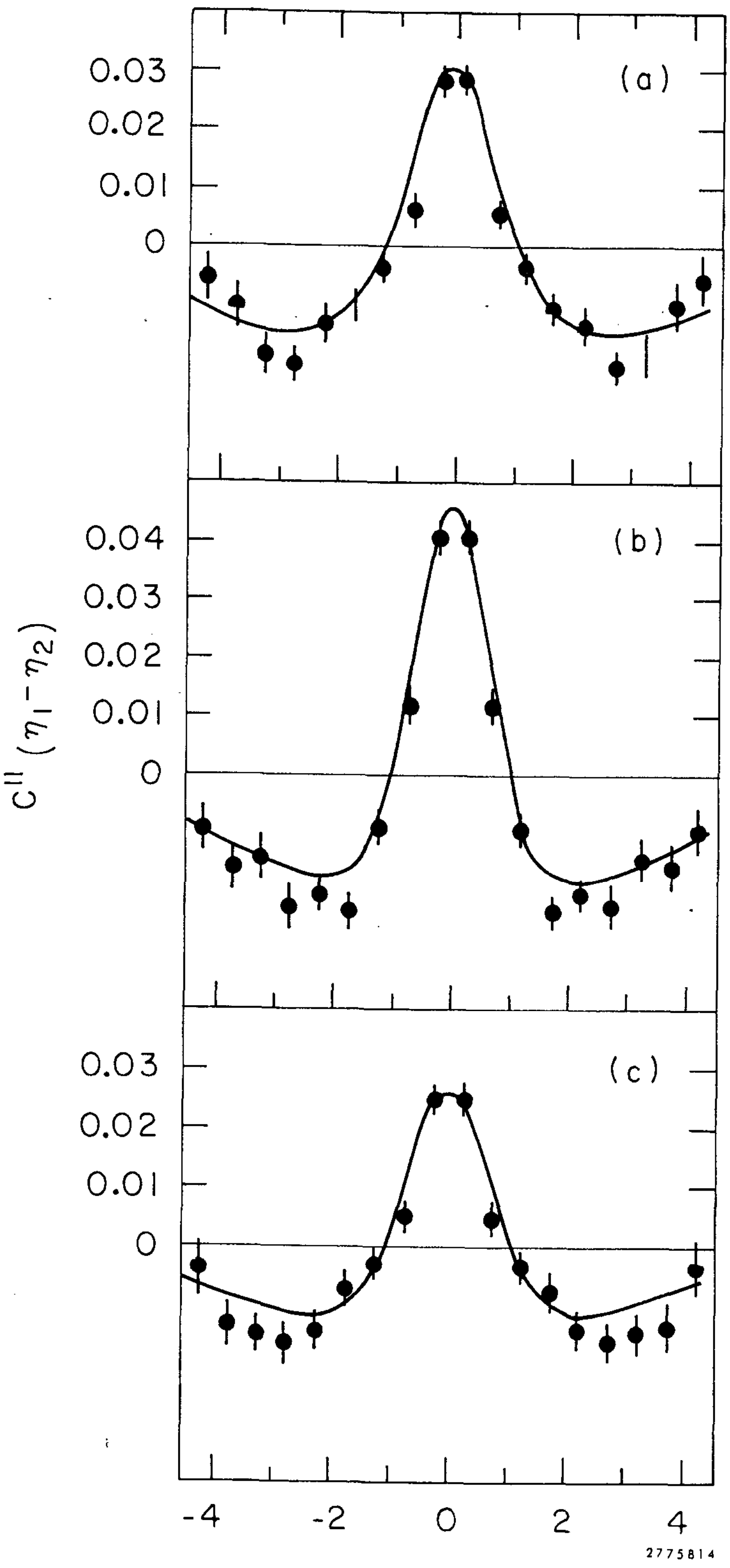

Fig. 14. Rapidity correlation functions between two charged particles produced centrally (a) in an interaction with no large $p_\perp$, (b) in the hemisphere of azimuths opposite to a trigger π^0 with $p_\perp \geq 2$ GeV, (c) in the hemisphere toward the trigger π^0. Data are from ACHM at $\sqrt{s} = 53$ GeV.

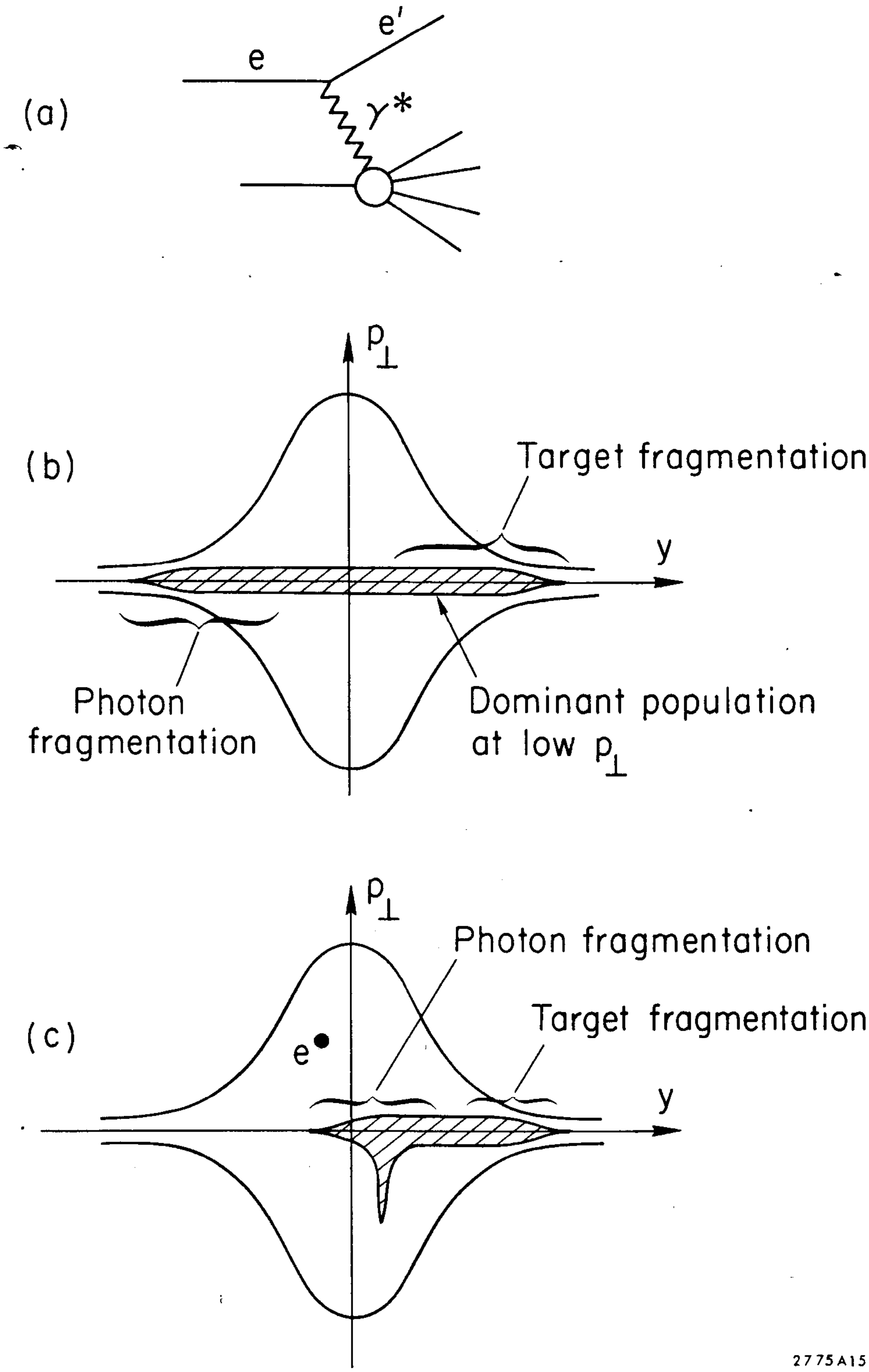

Fig. 15. (a) Diagram for hadron electroproduction; (b) Expected rapidity distribution of electroproduced hadrons in the laboratory frame, with z-axis along the virtual photon direction; (c) the same distribution mapped into the e-p CMS frame.

We can now consider the main prototype for a hard collision in pp interactions. This is via exchange of a highly virtual photon (Fig. 16a). The resulting rapidity distribution of produced hadrons (Fig. 16b) is evidently obtainable from Fig. 15. We see that the positions in y of the jet axes depend upon Q^2, ω_1, and ω_2, and can, at very large s/Q^2, vary over a wide interval.

In addition, suppose the inclusive distribution of electroproduced hadrons obeys Feynman scaling (or "limiting fragmentation"); that is (in the ordinary laboratory frame), the inclusive distribution of energetic hadrons obeys

$$z \frac{dN}{dz} = \frac{z}{\sigma} \frac{d\sigma}{dz} = g(z) \tag{3.1}$$

with $z = p_{\parallel}/p_{max}$. This maps into the statement that for the e-p cms kinematics, the high-$p_\perp$ hadrons obey a similar scaling law

$$p_\perp \frac{dN}{dp_\perp} = g\left(\frac{p_\perp}{p_\perp^{jet}}\right) \tag{3.2}$$

There is not much evidence regarding the validity of such scaling in high-$p_\perp$ collisions.

Finally, there is a scaling property of the inclusive distribution of high-$p_\perp$ hadrons which follows from the absence of any intrinsic energy scale in the supposed dynamics of the virtual photon exchange process:

$$E \frac{d\sigma}{d^3p} \sim p_\perp^{-4} f\left(\frac{p}{p_{max}}, \theta_{cm}\right) \tag{3.3}$$

While it might be natural to anticipate a similar behavior for the strong pp collisions, this does <u>not</u> occur, and if there <u>is</u> a scaling law, the exponent is approximately 8, not 4. In any event, the γ-exchange process has nothing to do

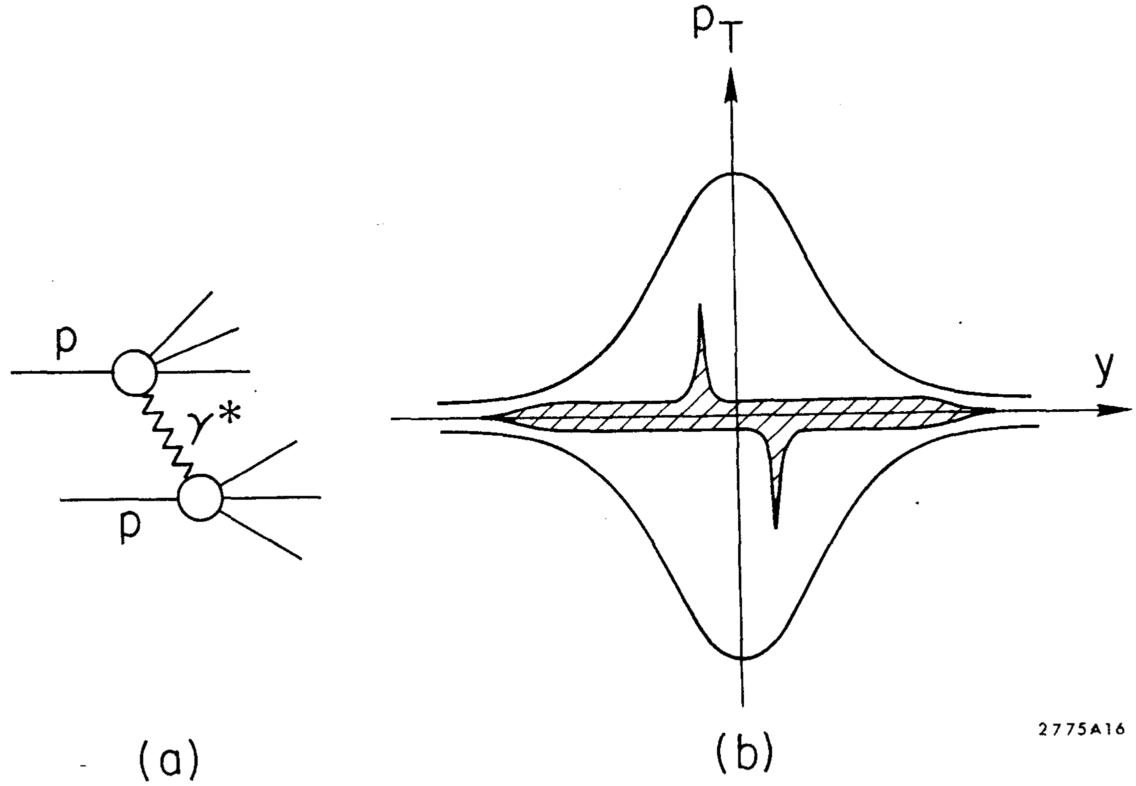

Fig. 16. (a) Diagram for $\bar{p}p$ interactions via photon exchange. (b) Rapidity distribution of produced hadrons for the photon-exchange process.

with the observed high-$p_\perp$ phenomena: it is too small by a factor of $\sim 10^4$. But it may still be of use as a prototype of the collisions we do observe—in terms of understanding the populations in phase-space of produced hadrons.

Up to now we have not needed to introduce the concept of constituents or partons to motivate the hard-collision hypothesis. However, if one accepts the notions of the parton model, then the leading hadrons ("photon fragments") in electroproduction become "parton fragments." When they are mapped into the phase-space appropriate for the pp collision, the parton fragments become the high-$p_\perp$ hadron jets. And the kinematics of the collision becomes much more transparent. Of course, in going over to the strong high-$p_\perp$ collisions, the whole question of the relevance of constituents has to be reexamined. And the constituents need not be point quarks: there are also gluons, diquarks, or other parton clusters ("mesons," "baryons"). We return to the question of what collides with what in Section VI.

IV. STATUS OF JETS IN LEPTON PHYSICS

This section is only a cursory review of the properties expected for hadrons produced in lepton-initiated processes. A more detailed discussion can be found in Gilman's lectures. What we need here are the broad features of the hadron distributions, to be used as input to the prototype hard-collisions discussed in the previous section. The lepton-induced processes for which we have some information are

$$\begin{cases} e^- p \to e^- \text{ hadrons} \\ \mu^- p \to \mu^- \text{ hadrons} \end{cases}$$

$$\nu p \to \mu^- \text{ hadrons}$$

$$e^+ e^- \to \text{hadrons}$$

In the parton model, the leading hadrons are "fragments" of a parton, and in particular the "up" quark should predominate in all reactions. Therefore, to a rough approximation, the distributions should obey Feynman scaling and all be the same. There is some evidence that this is not terribly far from the truth:

(a) Multiplicity. The multiplicity of produced hadrons seems to depend primarily on W, the total center-of-mass energy of the hadrons, independent of Q^2 and of process. In Fig. 17, we have plotted data from SLAC and Cornell for electroproduction,[4] SLAC data for colliding beams,[4] a quoted fit to ν - p data[5] from 15' hydrogen bubble chamber exposures at FNAL, and a rough fit to multiplicities observed in pp and πp collisions.

(b) Inclusive Spectra. For electroproduction, we have reconstructed the inclusive spectrum of leading charged hadrons dN_{ch}/dz from SLAC data,[6] and compared it (Fig. 18) with data from e^+e^- annihilation at $E_{cms} = 4.8$ GeV, as reported in the 1974 London Conference. The e^+e^- spectrum has been divided by two, inasmuch as two partons are produced, not one as in electroproduction. One sees general agreement at the factor-of-two level. We should probably not expect better, because of the "new physics," which provides half the e^+e^- events, but certainly not half the electroproduction events. In any case, there should be considerably more data presented at the Lepton-Photon Conference, along with careful comparisons of the spectra.

(c) $\langle p_\perp \rangle$ Relative to Jet Axis. Very recent data[7] (Fig. 19) from a University of California (Santa Barbara) experiment at SLAC indicate a sharp increase in the $\langle p_\perp \rangle$ of leading ($z > 0.4$) electroproduced π^0 as Q^2 increases. The trend is consistent with the earlier charged-particle data at SLAC and implies a $\langle p_\perp \rangle$ in excess of 1 GeV for $Q^2 \lesssim 5$ GeV^2. Can this be connected with the large $\langle p_N \rangle$ observed by CCR? This measurement deserves close analysis and confirmation,

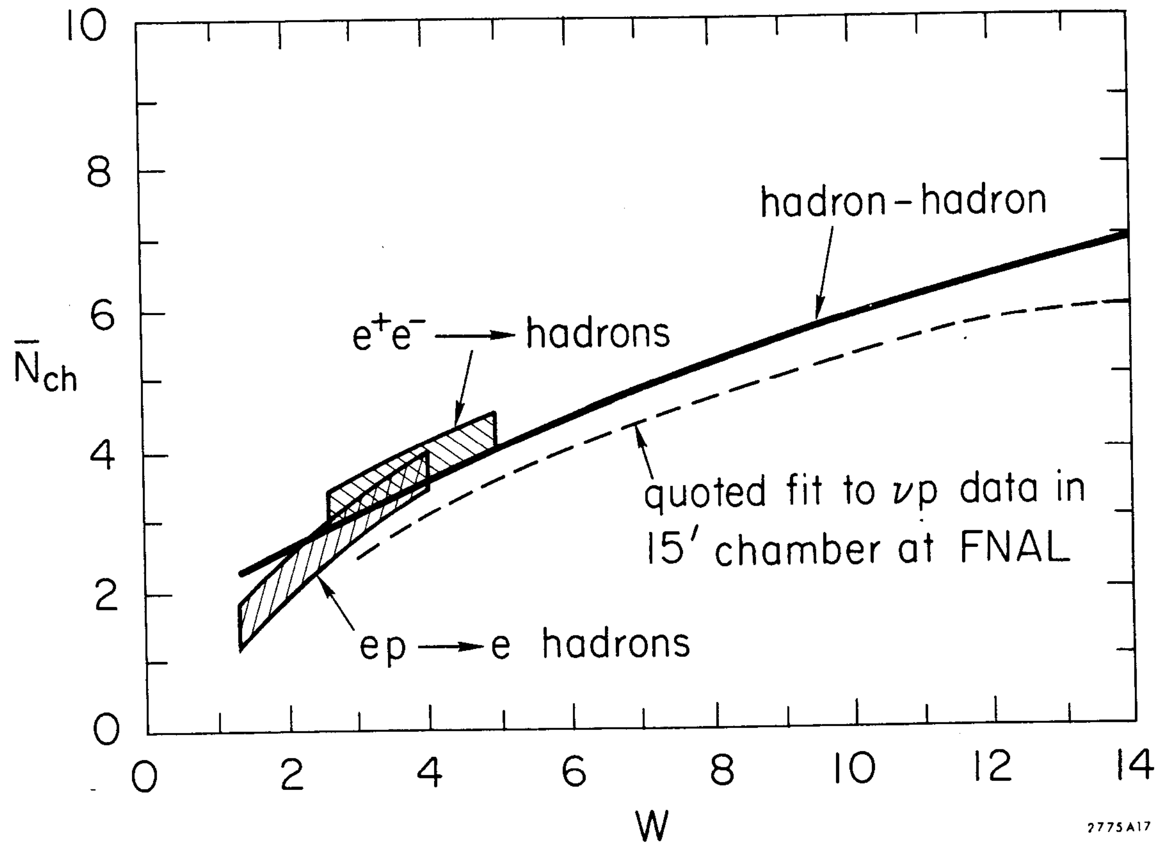

Fig. 17. Multiplicity of produced hadrons as function of the available hadron CMS energy W for various processes.

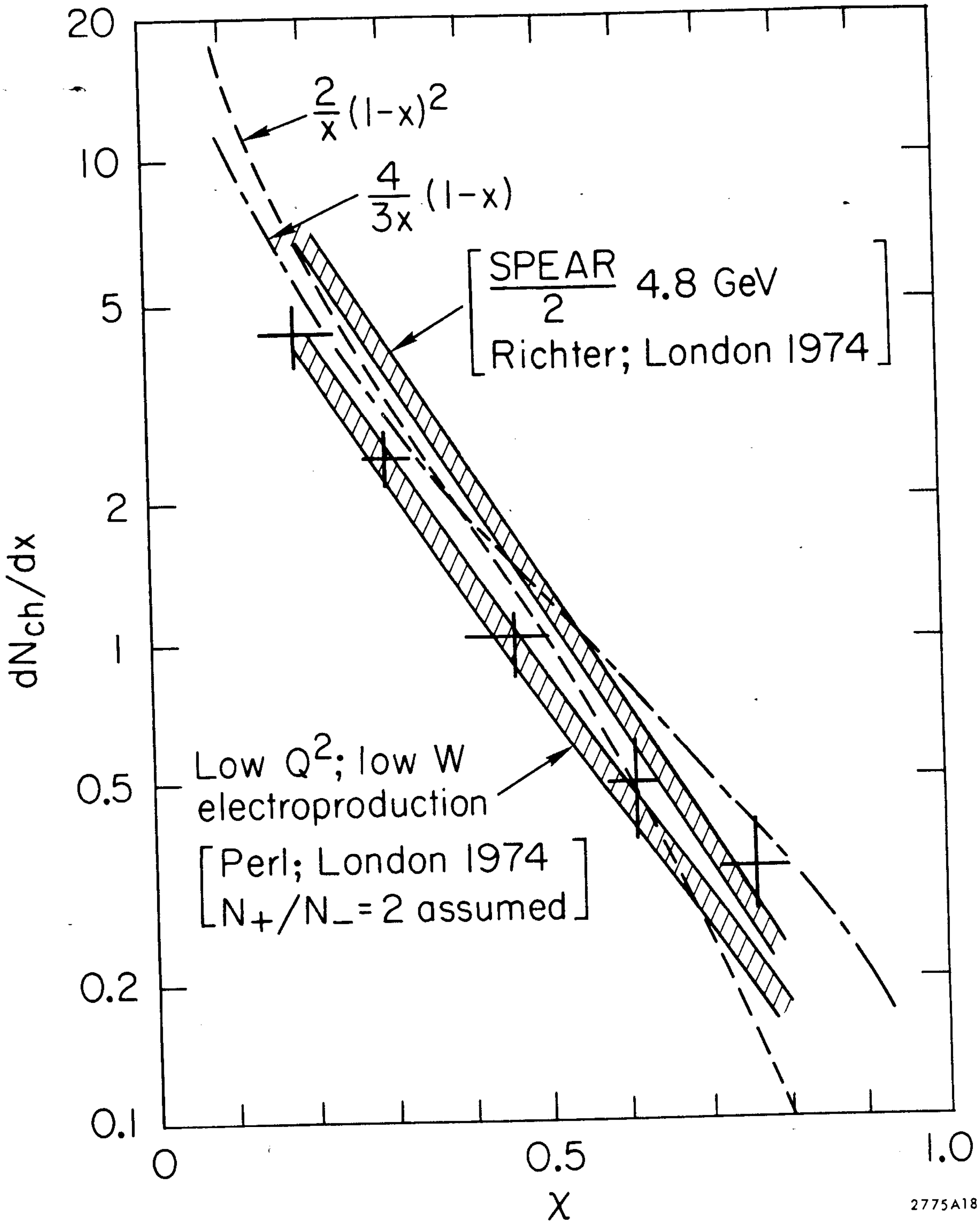

Fig. 18. Inclusive charged-hadron spectra in electroproduction and colliding-beam processes.

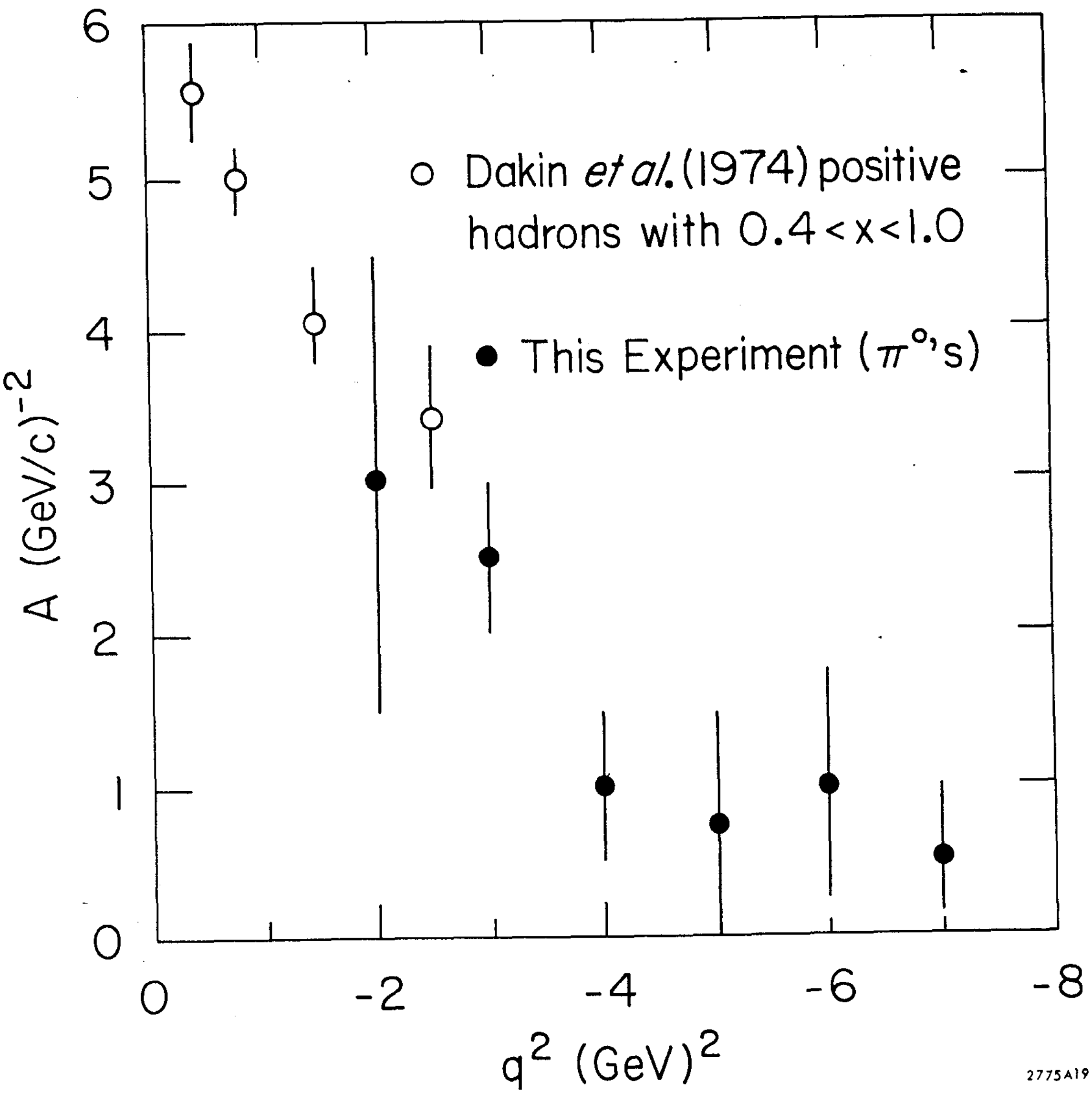

Fig. 19. Slope parameter in inclusive π^{o} electroproduction, as measured by UCSB for x > 0.4 GeV < $p_{\perp}$ $\lesssim$ 1.2 GeV, and 20 GeV electrons incident.

not only in electroproduction, but also in neutrino reactions. In addition, the relative $p_\perp$ between two opposite-side high-momentum ($z > 0.4$ again) hadrons produced in e^+e^- annihilation should be measured as well. Again, this question should be much clearer by the end of the summer.

However, despite this state of confusion, it would appear that something like the jets expected in the parton model do exist in lepton physics, with the outstanding issue (at the rough, factor-of-two level of accuracy) remaining being the $\langle p_\perp \rangle$ of leading hadrons relative to the jet axis. However, even if it turns out that for leading hadrons $\langle p_\perp \rangle \sim \sqrt{Q^2}$ in lepton physics, this will not necessarily make impossible the identification of jets in hadron-hadron collisions. It could only mean that, independent of the jet $p_\perp$, the high-$p_\perp$ hadrons in the jet would be found in a fixed solid angle interval surrounding the jet axis. Provided only that multiplicities stay low and Feynman scaling remains approximately true, one should still be able to identify the high-$p_\perp$ jets in hadron-hadron collisions (assuming, of course, the production of such jets has a dynamics similar to that of the prototype collisions we are discussing).

It hardly needs to be mentioned that the jet structure directly observed in e^+e^- annihilation, as reported by Gail Hanson at the Topical Conference, lends general support to the picture as well.

V. COMPARISON WITH HIGH-$p_\perp$ HADRON-HADRON PROCESSES

We now return to the three hard-collision hypotheses in Section II and try to compare in a more quantitative way:

A. Coplanarity. We saw that $\pi^0 - \pi^\pm$ correlations yielded a value of $\langle p_N \rangle \sim 0.5 - 0.6$ GeV, while CCR measured $\langle p_N \rangle \gtrsim 1.3$ GeV for $\pi^0 - \pi^0$ correlations. To estimate what is reasonable, we take opposite-side high-$p_\perp$ hadrons (from γ-exchange) with $p_{\perp 1} > p_{\perp 2}$ and write

$$\langle p_N^2 \rangle \lesssim \frac{\langle |\vec{p}_{\perp 1} \times \vec{p}_{\perp 2}|^2 \rangle}{\langle p_{\perp 1}^2 \rangle} \tag{5.1}$$

which is essentially the experimentally measured quantity. We may put the z-axis in the beam direction and the x-axis in the direction of the exchanged photon. Then

$$\langle p_N^2 \rangle \approx \frac{\langle (p_{x1} p_{y2} - p_{y1} p_{x2})^2 \rangle}{\langle p_{x1}^2 \rangle} \tag{5.2}$$

$$\approx \frac{\langle p_{x1}^2 \rangle \langle p_{y2} \rangle^2 + \langle p_{y1}^2 \rangle \langle p_{x2}^2 \rangle}{\langle p_{x1}^2 \rangle} = \langle p_y^2 \rangle \left(1 + \frac{\langle p_{x2}^2 \rangle}{\langle p_{x1}^2 \rangle} \right)$$

$$\simeq 2 \langle p_{y2}^2 \rangle = 2 \langle p_N^2 \rangle_{\text{electroproduction}} = \langle p_\perp^2 \rangle_{\text{electroprod}}$$

where $\langle p_\perp^2 \rangle_{\text{electroprod}}$ is evidently the quantity discussed in the previous section. We see that

$$\langle p_N \rangle \sim \langle p_\perp \rangle_{\text{electroprod}} . \tag{5.3}$$

With electroproduction data parameterized as

$$\frac{dN}{dp_\perp^2} \sim e^{-bp_\perp^2} \tag{5.4}$$

one finds (Fig. 17)

$$\begin{array}{ll} b \sim 4 - 6 & Q^2 < 4 \text{ GeV}^2 \\ \left[\langle p_\perp \rangle \sim 0.4 - 0.5 \text{ GeV} \right] & \text{charged secondaries} \end{array} \tag{5.5}$$

and

$$b \gtrsim 1 \qquad\qquad Q^2 > 4$$
$$\left[\langle p_\perp \rangle > 1\ \mathrm{GeV}\right] \qquad\qquad \pi^0 \text{ secondaries} \tag{5.6}$$

Given the two ISR measurements of $\langle p_N \rangle \gtrsim 0.5$ GeV and $\langle p_N \rangle \gtrsim 1.3$ GeV, one may draw a variety of conclusions. The safest is that, at least for the near future, the matter rests in the hands of the experimentalists.

C. Opposite-Side Jet and its Inclusive Spectrum. We skip to the third hypothesis in an attempt to first ascertain the nature of jets produced in hadron-hadron collisions. There are three sources of information:

(i) There are CCR opposite-side π^0-π^0 correlation measurements,[2] which have rather large uncertainties, and which I here ignore.

(ii) CERN-SFM present normalized spectra of all high-$p_\perp$ opposite-side particles.

(iii) CCRS present spectra, not normalized, for particles emitted into a small solid angle (at $\theta^* = 90^0$) opposite the triggering particle.

CERN-SFM present dN_{ch}/dx integrated over a broad swath of rapidity of the charged opposite-side particle. x is defined as the ratio of the charged particle $p_\perp$ to the $p_\perp$ of the triggering π^0. When presented in this way, the data agree quite nicely (including normalization) with SLAC electroproduction data. Their presentation of the data is in Fig. 20.

It may be that a better variable than x is $x_J = p_{\perp 2}/p_{\perp\,\mathrm{jet}}$. As will be estimated in the next subsection, probably $p_{\perp\,\mathrm{jet}} \sim 1.3\ p_{1\perp}$. Then dN/dx gets rescaled a factor 1.3 horizontally as well as vertically $\left(\frac{dN}{dx_J} \approx 1.3\ \frac{dN}{dx}\right)$. This tends to move the experimental points below the electroproduction distribution, but the effect is not large.

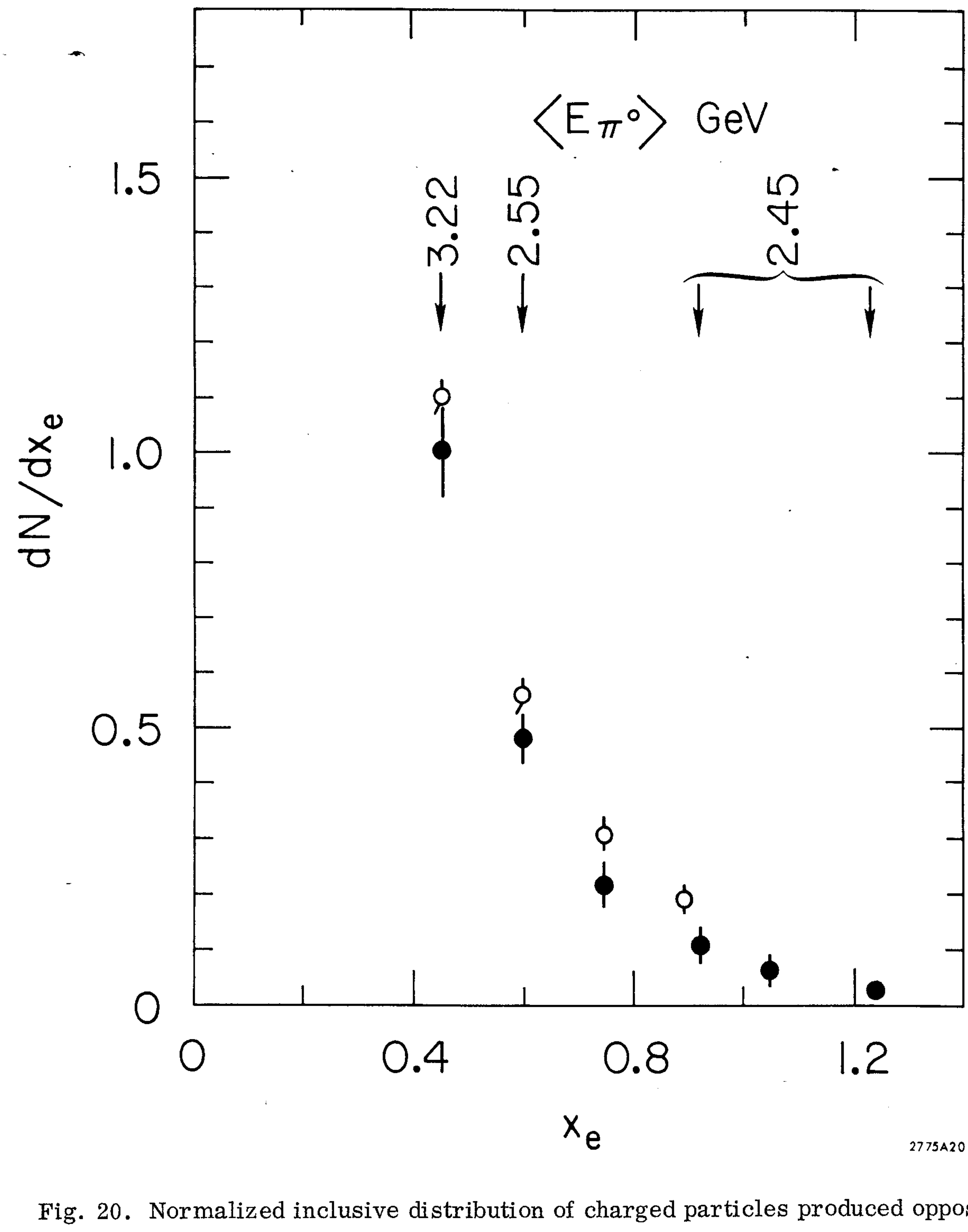

Fig. 20. Normalized inclusive distribution of charged particles produced opposite to a trigger π^o with 2.5 GeV $< p_\perp <$ 3.4 GeV. Data are from CERN-SFM. The solid points are electroproduction spectra for comparison.

In comparing the CCRS data with CERN-SFM, we note that what is measured by CCRS is a conditional inclusive spectrum.

$$F(p_2,\ldots) = \left. \frac{E_1 E_2 \dfrac{d\sigma}{d^3p_1\, d^3p_2}}{E_1 \dfrac{d\sigma}{d^3p_1}} = E_2 \frac{d\sigma}{d^3p_2} \right|_{\pi^0 \text{ trigger}}$$

$$= \left. \frac{d\sigma}{dy_2\, dp_{2\perp}\, dp_N} \right|_{\pi^0 \text{ trigger}} \tag{5.7}$$

where p_1 = trigger π^o momentum

p_2 = opposite-side charged particle momentum

Then

$$\frac{d\sigma}{dp_{2\perp}} = F(p_2)\ \langle \Delta y \rangle \ \langle p_N \rangle = (\text{const})\ F(p_2) \tag{5.8}$$

if we use the evidence from CERN-SFM that $\langle \Delta y \rangle$ and $\langle p_N \rangle$ are approximately constant. Assuming this is so, we have placed, in Fig. 21, the CCRS data against the CERN-SFM, normalizing the former to the latter in the overlap region. It would appear that the structure of the opposite-side jet (provided it exists!!) is at the least quite similar to what is seen in lepton-induced processes.

In Fig. 22 is plotted a crude estimate of the opposite-side excess multiplicity in comparison with the multiplicity found in lepton-induced processes. It may be a little larger, but the uncertainties are large and in any case, the magnitude of the discrepancy is nothing to be alarmed about.

B. Same-Side Jet. The consistency of the opposite-side high-$p_\perp$ hadron spectrum with that of a "jet" with properties similar to that of lepton-induced jets suggests the hypothesis that the same-side high-$p_\perp$ system is a similar jet.

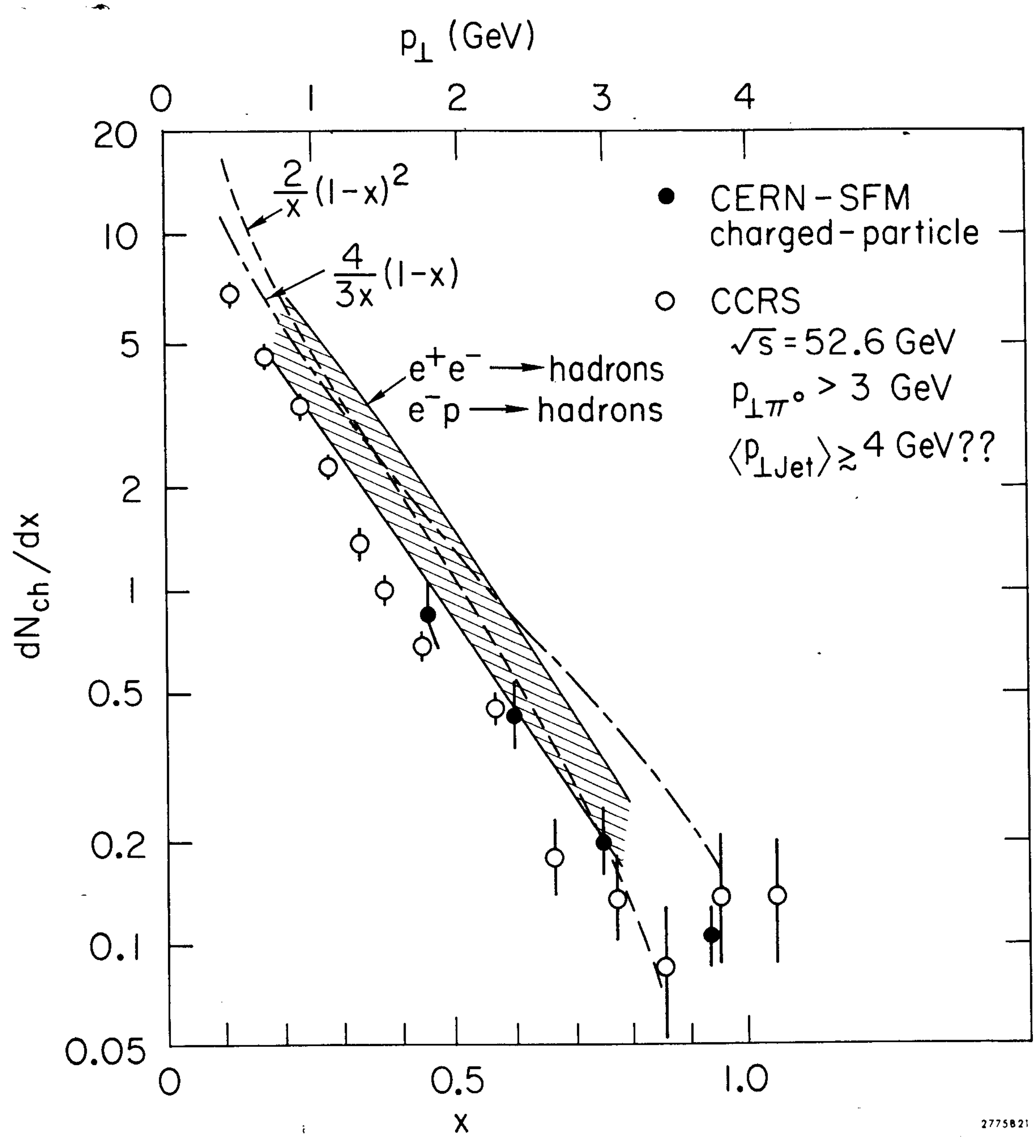

Fig. 21. The same data, compared against the inclusive spectrum presented in Fig. 18. Also shown are the CCRS data, normalized to agree with CERN-SFM in the overlap region. The horizontal scale of CCRS (shown on the top) is chosen so that $x = p_\perp / p_{\perp\pi^0}$. See the text for a critique of this choice.

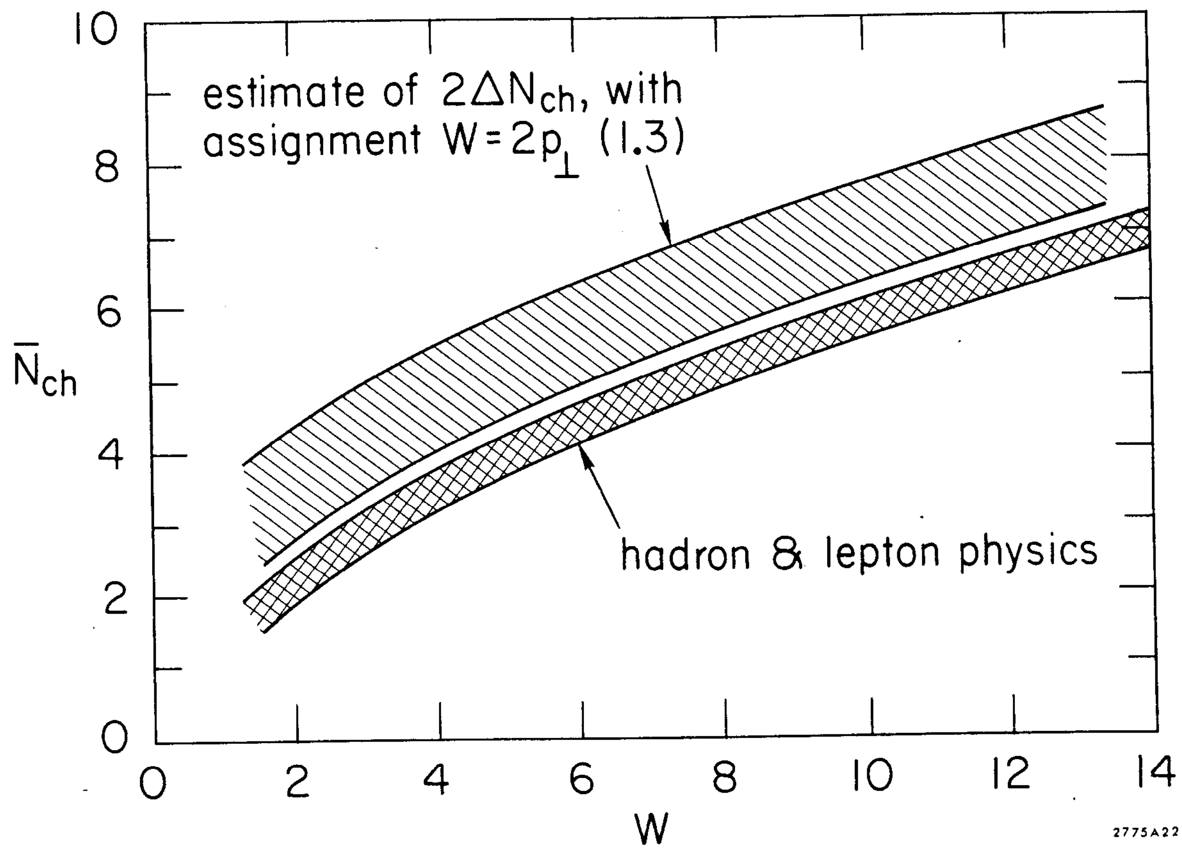

Fig. 22. Estimate of twice the excess multiplicity (of the opposite side produced particles) vs W $\approx$ 2.6 $p_{\perp 1}$ (the estimated total CMS energy of the high-$p_\perp$ system), in comparison with lepton-induced processes.

However, before testing such a hypothesis, the bias induced by the existence of the high-$p_\perp$ trigger particle must be understood.

To do this, assume the triggering π^o is the product of a jet, which has a production spectrum

$$\frac{d\sigma}{d\,p_{\perp\,(\mathrm{Jet})}} = C\,p_{\perp\,(\mathrm{Jet})}^{-n_{\mathrm{eff}}\,(p_\perp)} \tag{5.9}$$

which is roughly similar in shape to the inclusive spectrum. Experimentally, (Fig. 23), $n_{\mathrm{eff}} \lesssim 8 \pm 1$ at ISR energies ($\sqrt{s} \sim 45$ GeV) and varies slowly with $p_\perp$ (once $p_\perp \gtrsim 3$ GeV).

We now suppose the conditional inclusive π^o spectrum is similar in shape to the charged spectra. For that, we take a reasonable average to be

$$\frac{d\,N_{ch}}{d\,x} \sim 20\;e^{-5.6x} \tag{5.10}$$

so that

$$\frac{d\,N\pi^o}{d\,x} \cong 10\;e^{-5.6x} \equiv f\,(x) \tag{5.11}$$

where

$$x = p_\perp / p_{\perp\,\mathrm{Jet}}$$

Thus

$$\begin{aligned} \frac{d\sigma_{\pi^o}}{d\,p_\perp} &\approx \int_{p_\perp}^{\infty} \frac{d\,p_{\perp\,\mathrm{Jet}}}{p_{\perp\,\mathrm{Jet}}} \left(\frac{d\sigma}{d\,p_{\perp\,\mathrm{Jet}}}\right) f\,(x) \\ &= \int_0^1 \frac{d\,x}{x}\, C \left(\frac{x}{p_\perp}\right)^{n_{\mathrm{eff}}} f\,(x) \end{aligned} \tag{5.12}$$

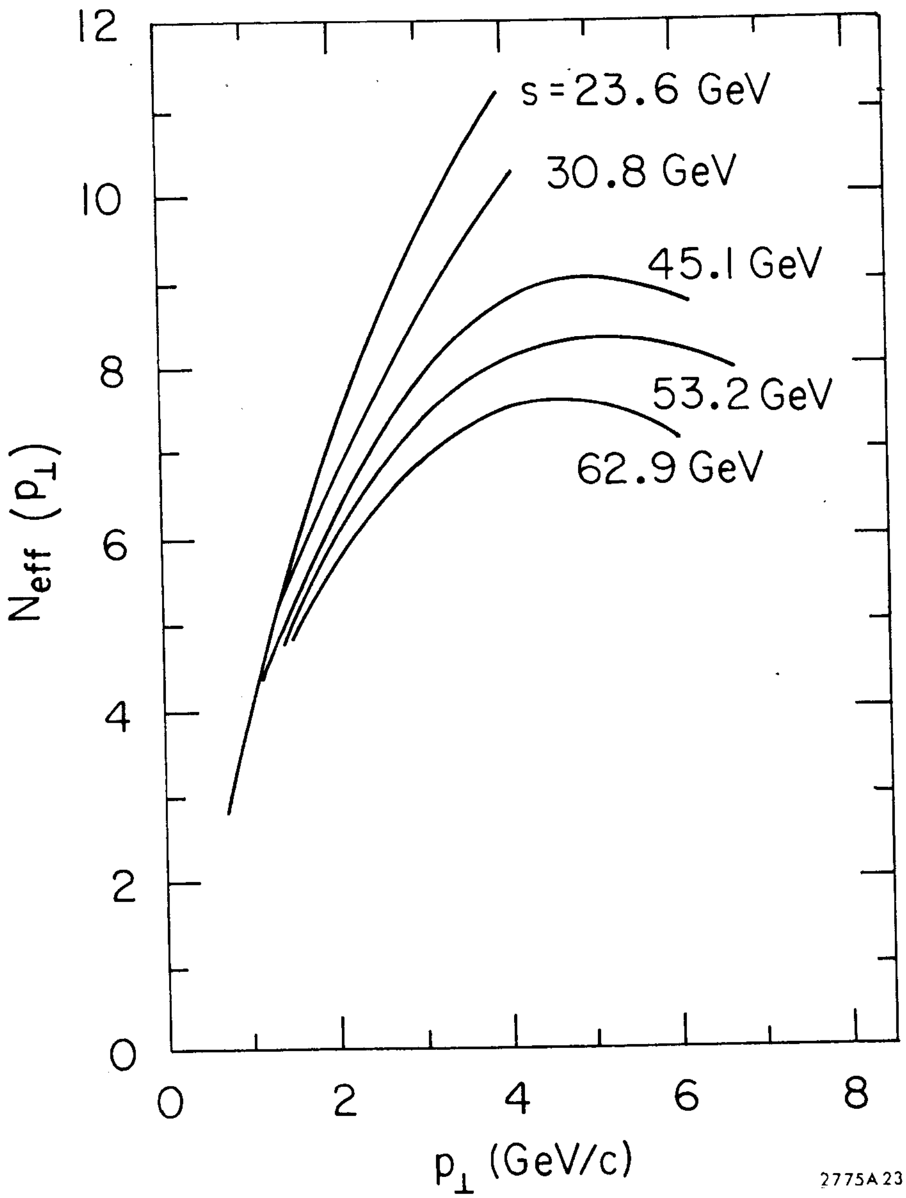

Fig. 23. Local exponent $n_{eff} = \frac{-p_\perp}{\sigma} \frac{d\sigma}{dp_\perp}$ vs $p_\perp$. Taken from Darriulat's review talk at Palermo Conference.

Given $n_{eff} \approx$ constant, we find the ratio of π^o/Jet at the same transverse momentum to be

$$\frac{\pi^o}{\text{Jet}} = \left(\frac{d\sigma}{dp_\perp}\right)_{\pi^o} \Big/ \left(\frac{d\sigma}{dp_\perp}\right)_{\text{Jet}} = \int_0^1 dx\, x^{n_{eff}-1} f(x) \qquad (5.13)$$

The integrand is plotted in Fig. 24. We see that it is not too sensitive to n_{eff}, but that it is quite sensitive to the behavior of f(x) for $x > 0.8$, where measurements are sparse and in any case difficult to interpret. Thus the area is certain to no better than a factor 2, but the nominal ratio is

$$\frac{\pi^o}{\text{Jet}} = 2.2\% \qquad (5.14)$$

In any case, the mean value of x is $\sim .75 - .85$. Thus, with the trigger-π^o carrying 3/4 of the total $p_\perp$, the composition of the same-side jet is very atypical. (A "typical" jet could, in principle, be obtained by triggering on large total $p_\perp$ deposited into a given solid angle, e.g., by use of a hadron calorimeter.)

We may now generalize the previous calculation to estimate the joint distribution of two π's, say one π^o and one π^-, both of high $p_\perp$ and emerging together on the same side. We shall assume small correlation of the two pions <u>within</u> the jet, as is the case in ordinary hadron-hadron processes. We write

$$\frac{dN}{dx_1\, dx_2} = \frac{dN}{dx_1}\, \frac{dN}{dx_2}\, R(x_1, x_2) \qquad (5.15)$$

where $x_i = p_{\perp i}/p_{\perp \text{Jet}}$ and $R = 1 + C$, with C the correlation function. For the relevant x-interval ($x_1 + x_2 \sim 0.7$), we take $0 \le C \le 1$, an assumption which appears not to be in conflict with what is observed in ordinary processes. We

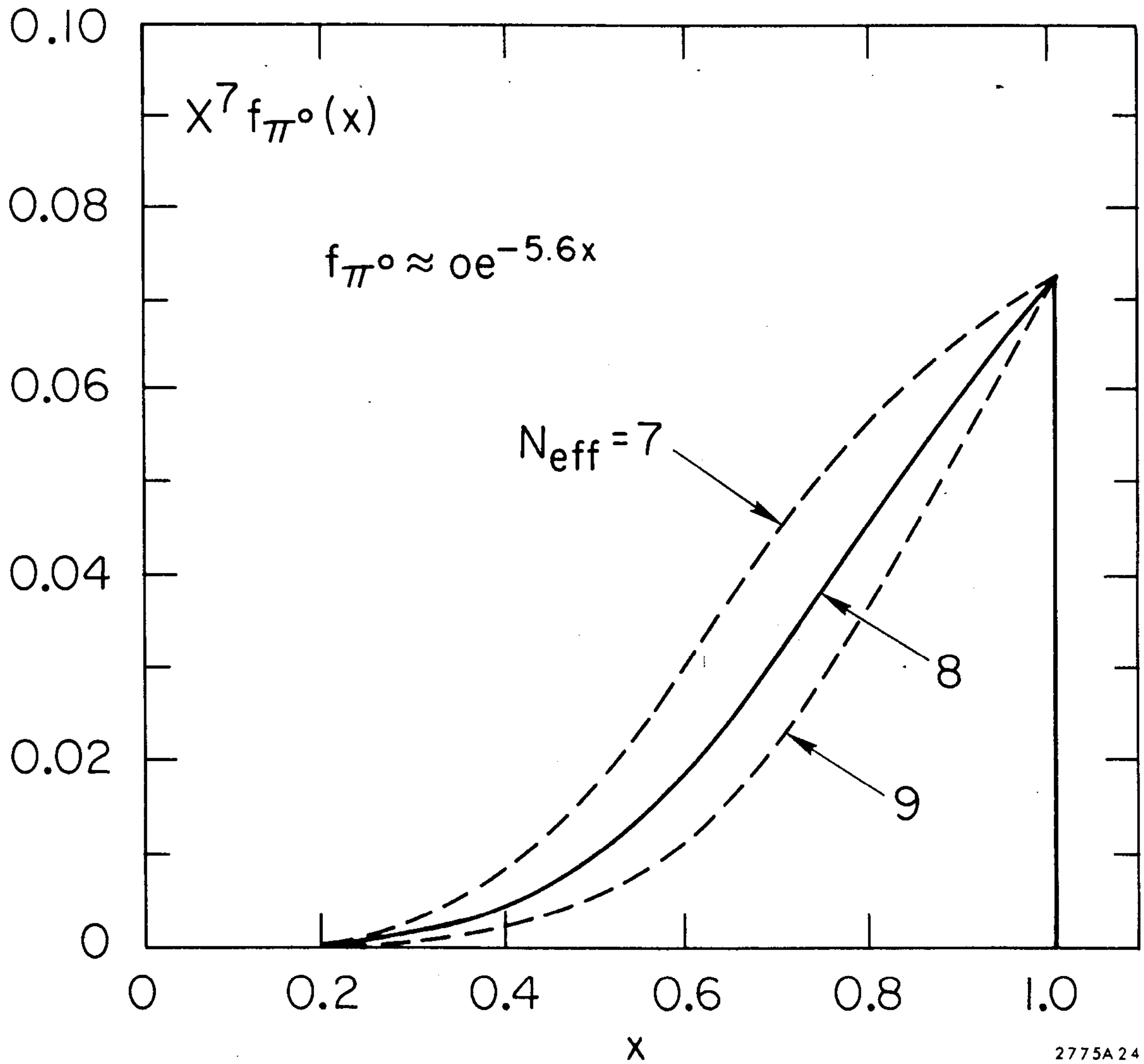

Fig. 24. Integrand for Eq. (5.13) vs x.

may now fold this distribution over the production spectrum of the jets as before:

$$\frac{d\sigma}{dp_{1\perp}\, dp_{2\perp}} \int_{p_{1\perp}+p_{2\perp}}^{\infty} \frac{dp_{\perp\,\mathrm{Jet}}}{p^2_{\perp\,\mathrm{Jet}}} \left(\frac{C}{p_{\perp\,\mathrm{Jet}}^{n_{\mathrm{eff}}}}\right) f(x_1)\, f(x_2)\, \overline{R} \qquad (5.16)$$

Some changes of variables expedite the integration. We let

$$\epsilon = \frac{p_{2\perp}}{p_{1\perp}+p_{2\perp}} = \frac{p_{2\perp}}{p_\perp} \qquad (p_\perp = p_{\perp 1} + p_{\perp 2}) \qquad (5.17)$$

be the fraction of dipion momentum $p_\perp$ given to pion no 2. Then with the definition $x = p_\perp / p_{\perp\,\mathrm{Jet}}$, and the observation that, for the exponential form chosen to approximate f(x),

$$f(x_1)\, f(x_2) = f(0)\, f(x_1 + x_2) = f(0) f(x) \qquad (5.18)$$

we obtain the inclusive spectrum of dipions of <u>total</u> transverse momentum $p_\perp$

$$\frac{d\sigma}{dp_\perp\, d\epsilon} = \left(\frac{C}{p_\perp^{n_{\mathrm{eff}}}}\right) f(0)\, \overline{R} \int_0^1 dx\, x^{n_{\mathrm{eff}}}\, f(x) \qquad (5.19)$$

This integral has one power more of n_{eff} than the previous one; inspection of Fig. 24 indicates it is ~ 0.8 as large. Then the ratio of pairs to single π^0's is

$$\frac{(\pi^0\pi^-)}{\pi^0} \equiv \frac{\left(\dfrac{d\sigma}{dp_\perp\, d\epsilon}\right)_{\pi^0\pi^-}}{\left(\dfrac{d\sigma}{dp_\perp}\right)_{\pi^0}} \approx 0.8\, f(0)\, \overline{R} \sim 8 - 16 \qquad (5.20)$$

The ϵ-dependence has, to some extent, been measured by ACHM; there is no dependence discerned for $\frac{1}{3} \lesssim \epsilon \lesssim \frac{2}{3}$ (cf Fig. 25).

We may also extract this same quantity from the measurements, in particular the ACHM same-side $\pi^o\pi^o$ measurements. We check by using two different strategies:

(i) Define

$$F_2 = E_1 E_2 \left. \frac{d\sigma}{d^3p_1 \, d^3p_2} \right|_{\pi^o\pi^o}$$

$$F_1 = E_1 \left. \frac{d\sigma}{d^3p_1} \right|_{\text{single } \pi^o} \tag{5.21}$$

Let

$p_\mu = p_{1\mu} + p_{2\mu}$ = dipion 4-momentum

m = dipion mass

ϵ = fraction of momentum given to particle 2 (as before)

ϕ = azimuthal angle of dipion relative to $p_\perp$ vector of dipion.

Then a straightforward change of variables gives

$$F_2 = 2E \frac{d\sigma}{d^3p \, dm^2 \, d\epsilon \, d\phi} \tag{5.22}$$

In presenting their data, ACHM averages over m^2, ϵ, and ϕ:

$$\left\langle E \frac{d\sigma}{d^3p \, d\epsilon} \right\rangle \sim \pi \langle F_2 \rangle \langle \Delta m^2 \rangle \tag{5.23}$$

and the dipion/pion ratio previously defined becomes

$$\frac{(\pi^o\pi^o)}{\pi^o} = \frac{\left(E \frac{d\sigma}{d^3p \, d\epsilon} \right)_{\pi^o\pi^o}}{\left(E \frac{d\sigma}{d^3p} \right)_{\pi^o}} \approx \pi \frac{\langle F_2 \rangle}{F_1} \langle \Delta m^2 \rangle \tag{5.24}$$

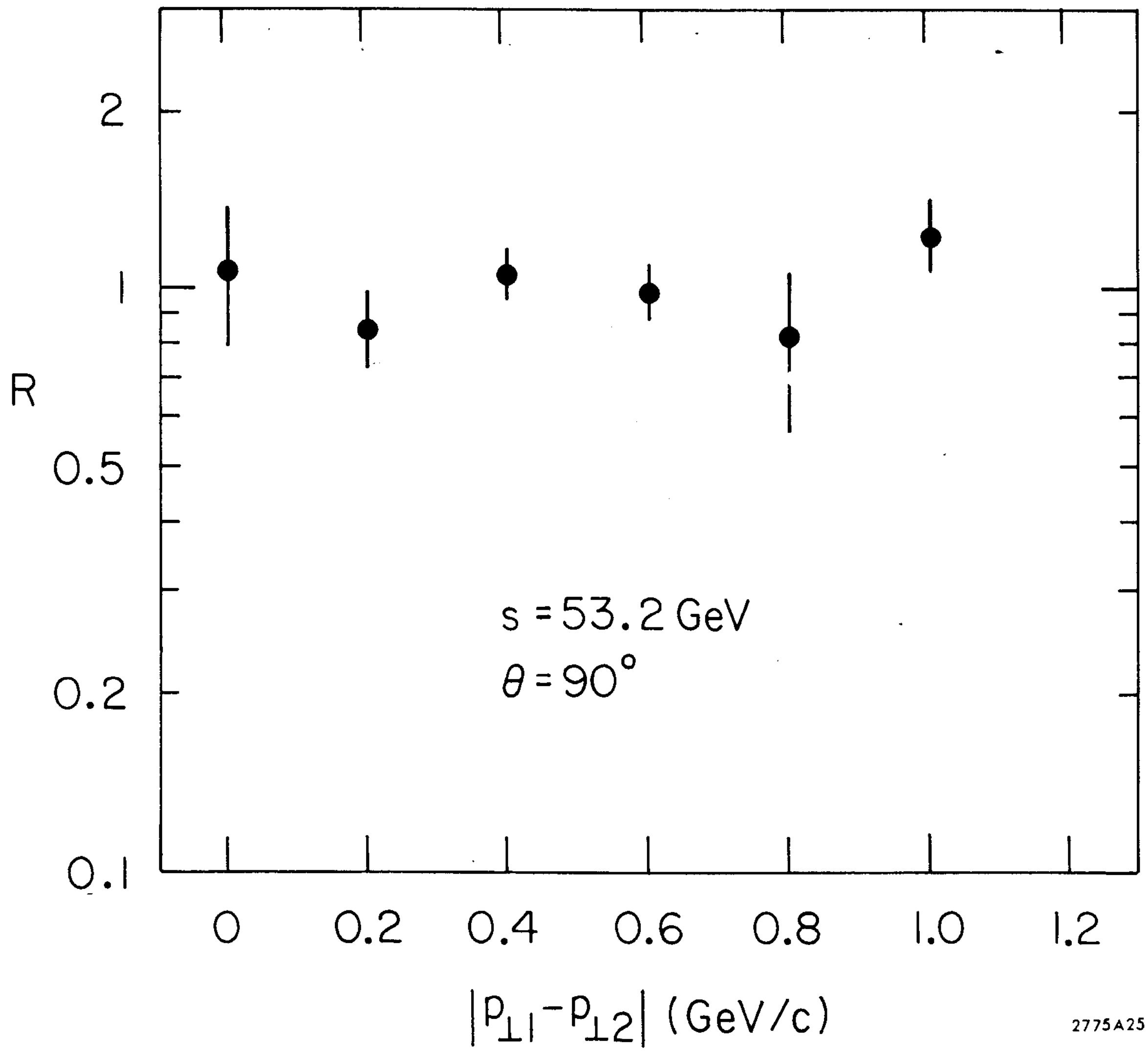

Fig. 25. Dependence of the yield at fixed $p_\perp = |p_{\perp 1} + p_{\perp 2}|$ ($\gtrsim 3$ GeV) on $|p_{\perp 1} - p_{\perp 2}| = (1 - 2\epsilon)p_\perp$. Data are from ACHM.

$\frac{\langle F_2 \rangle}{F_1}$ is quoted by ACHM; from their paper, one obtains $\frac{F_2}{F_1} \sim 4.5\ \mathrm{GeV}^{-2}$ for $5 < p_\perp < 8$ GeV and $\sqrt{s} = 52.6$ GeV. The first conclusion is, of course, that the prediction of approximate constancy of the $(\pi\pi)/\pi$ ratio with $p_\perp$ is consistent with the data. Using $\langle \Delta m^2 \rangle \sim 1.1\ \mathrm{GeV}^2$ from the CERN-SFM data, we get

$$\frac{(\pi^o \pi^o)}{\pi^o} \sim 15 \tag{5.25}$$

(ii) We may also write

$$F_2 = \frac{d\sigma}{dy_1\, dy_2\, dp_\perp\, dp_{\perp 2}\, dp_{N1}\, dp_{N2}}$$

$$\sim \frac{1}{2\, \langle \Delta p_{N2} \rangle \langle \Delta y_2 \rangle} \qquad \frac{d\sigma}{dy_1\, dp_\perp\, p_\perp\, d\epsilon\, dp_{N1}} \tag{5.26}$$

(The factor 2 comes from integration over p_{N2} from $-\infty$ to $+\infty$.)

Likewise

$$F_1 = \frac{d\sigma}{dy_1\, dp_{N1}\, dp_\perp} \tag{5.27}$$

and thus

$$\left(\frac{\pi^o \pi^o}{\pi^o}\right) = \frac{\left(\frac{d\sigma}{dy_1\, dp_{N1}\, dp_\perp\, d\epsilon}\right)}{\left(\frac{d\sigma}{dy_1\, dp_{N1}\, dp_\perp}\right)} = 2 p_\perp \langle \Delta p_N \rangle \langle \Delta y_2 \rangle \frac{F_2}{F_1} - \tag{5.28}$$

For $p_\perp \sim 6 \pm 2$ GeV, ACHM observes (Fig. 8) $\Delta y_2 \sim 1$. (Notice also that for "standard" jets $\langle \Delta y \rangle\, p_\perp \sim$ constant independent of $p_\perp$.) Then putting in $\langle p_{N1} \rangle \sim \frac{0.5\ \mathrm{GeV}}{\sqrt{2}} \sim .35$ GeV and the observed $F_2/F_1 \sim 4.5$, we recover

$$\frac{(\pi^o \pi^o)}{\pi^o} \sim 18 \tag{5.29}$$

There is at least good compatibility between the two estimates. Also the general compatibility of the dipion/pion ratio with the theoretical estimate (and especially its constancy with $p_\perp$) lends support (but not proof) that the same-side high-$p_\perp$ system is a jet with properties not dissimilar to those of the opposite-side jet. Furthermore, there appear to be enough dipions ($\pi^\pm \pi^0 + \pi^+ \pi^- + \pi^0 \pi^0$ gives $\sim 4 \cdot 15 \sim 60\, \pi^0$!!) to account for the majority of the "jets" required by Eq. (5.14).

However, one cannot rule out other interpretations. For example, in the constituent interchange model (discussed mainly in Michel Davier's lectures), the basic subprocess believed relevant to the 90° CMS ISR spectra is quark-meson scattering. This implies that the opposite-side system is a quark jet, while the same-side system is a "meson," presumably of low mass. Whether the large, low mass dipion continuum can be regarded as decay products of unstable "mesons" remains an open question.

We may finally study the same-side conditional inclusive spectrum measured by CCRS (Fig. 5). If indeed $(\pi\pi)/\pi$ = constant, it follows from Eq. (5.21) that

$$\frac{E_1 E_2 \dfrac{d\sigma}{d^3p_2\, d^3p_1}}{E_1 \dfrac{d\sigma}{d^3p_1}} = \frac{F_2(p_1+p_2)}{F_1(p_1)} = (\text{const})\, \frac{F_1(p_1+p_2)}{F_1(p_1)} \tag{5.30}$$

While the CCRS data is not normalized, the s-dependence should be visible. The trigger π^0 momentum p_1 is restricted to be larger than 3 GeV. We take $p_1 \sim 4$ GeV and plot in Fig. 26 the expected behavior of F_2/F_1 with $\sqrt{s}$. It is certainly consistent with experiment.

Hence the same-side correlation data all seems to be internally consistent and quite consistent with hard-collision hypotheses, including the supposition that the same-side jet also shares the general properties of the opposite-side jet and of lepton-induced jets.

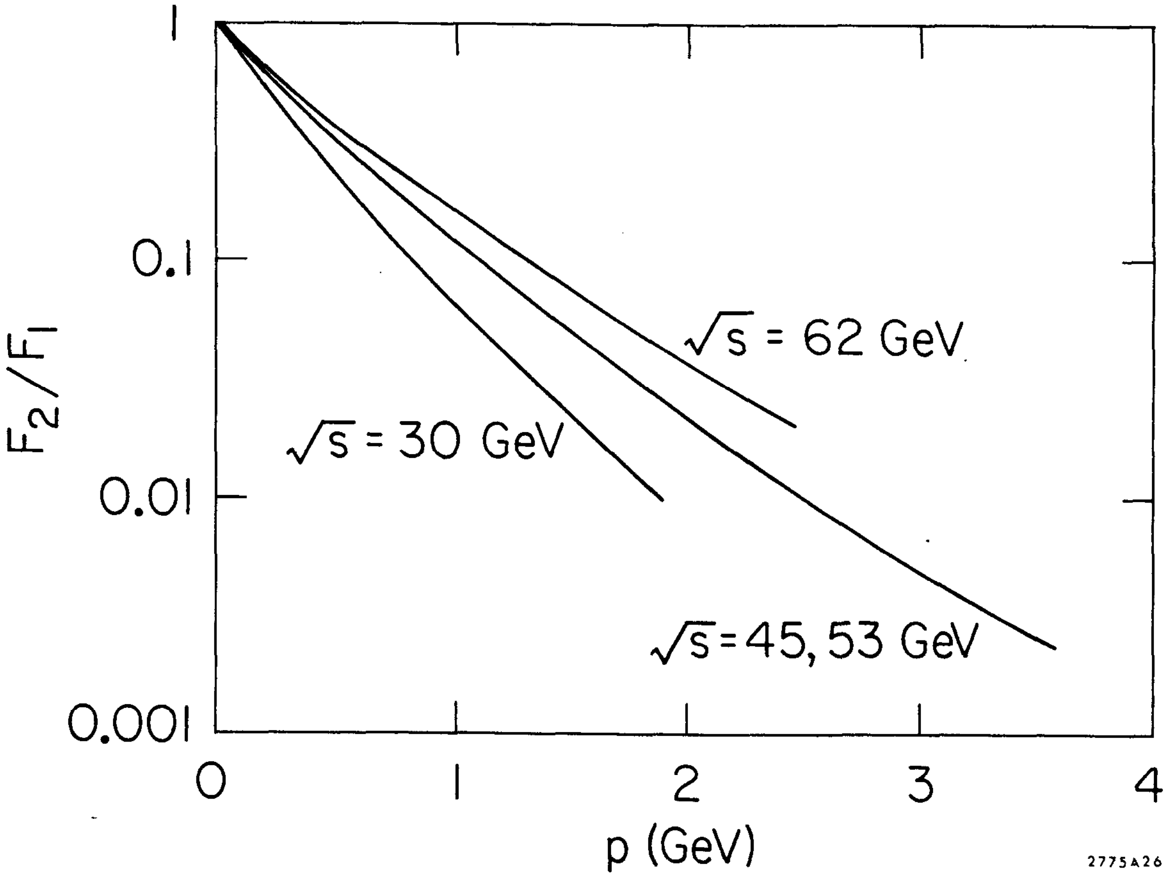

Fig. 26. Expected behavior of same-side inclusive spectrum with $\sqrt{s}$ under the hypothesis that $(\pi\pi)/\pi$ = constant.

VI. SOME COMMENTS ON MORE SPECIFIC MODELS

In the previous section, we saw that the hard-collision hypotheses seem to be in general agreement with most correlation data, although one cannot claim that they are confirmed. However, for the present, let us suppose they are confirmed and address the main question:

WHAT'S GOING ON?

First of all, there is the question of whether the general hypotheses for phase-space populations that have been discussed really imply binary collisions of constituents residing in the incident projectiles. While the implication is strong, it is only an implication. Maybe the best test of the concept will be the test of time: either it remains of value or it doesn't. In any case, we do not consider here any alternatives.

Then all that is left are the answers to the following simple questions:

(i) What are the incident constituents a and b of projectiles A and B which undergo the hard collision?

(ii) How do constituents a and b collide, and what is the differential cross section $d\sigma/dt$??

(iii) What are the outgoing constituents c and d after the binary collision?

(iv) How do constituents c and d fragment (if at all) into the observed high-$p_\perp$ hadron systems C and D??

There are a variety of candidates for initial and final constituents, which include quarks, antiquarks, gluons (including strings or bags), diquarks, triquarks (i.e., baryons), quark-antiquarks ("mesons"), the new partons (e.g., charmed quarks), or the new particles (e.g., charmed hadrons). We shall consider in turn the possible role of each such constituent:

A. Quarks and Antiquarks as Beam Constituents.

There is a constraint on how much antiquark is present in the incident projectiles from the ratio $\sigma_{\bar{\nu} N}/\sigma_{\nu N} \sim \frac{1}{3}$ measured in neutrino processes. For the scaling variable $x \gtrsim 0.1$, a reasonable bound is

$$\frac{\left(\frac{dN}{dx}\right)_{\bar{q}}}{\left(\frac{dN}{dx}\right)_{q}} \ll \frac{1}{3} \tag{6.1}$$

Inasmuch as most high-$p_\perp$ data requires the longitudinal fraction of the constituents to be $\gtrsim 0.1$, this implies that any collision mechanism that relies upon

$$\frac{q\bar{q} \rightarrow cd}{qq \rightarrow cd} \gg 1 \tag{6.2}$$

and which contributes significantly to the yields in pp collisions will contribute overwhelmingly for πN collisions under the same conditions. That is

$$\frac{\pi N \rightarrow cd + \ldots}{NN \rightarrow cd + \ldots} \gg 1 \tag{6.3}$$

simply because the π contains a valence antiquark, not possessed by the N.

Measurements of such production ratios at FNAL should be a good constraint on production mechanisms involving antiquarks as initial constituents.

Another possible problem with mechanisms specific to $q\bar{q}$ processes may be that the opposite-side rapidity correlations may be wrong. For a $q\bar{q}$ annihilation mechanism, there is a strong tendency for the opposite-side jet to have the same rapidity as the same-side trigger. This configuration both minimizes the subenergy s' for the hard annihilations, and minimizes the longitudinal fraction $\bar{x}$ of the antiquark in the initial beam (cf Fig. 27). However, data from ACHM, as well as unpublished data from DLR, indicate that if the pion trigger has positive rapidity, the opposite-side particles tend to be emitted at negative rapidities.

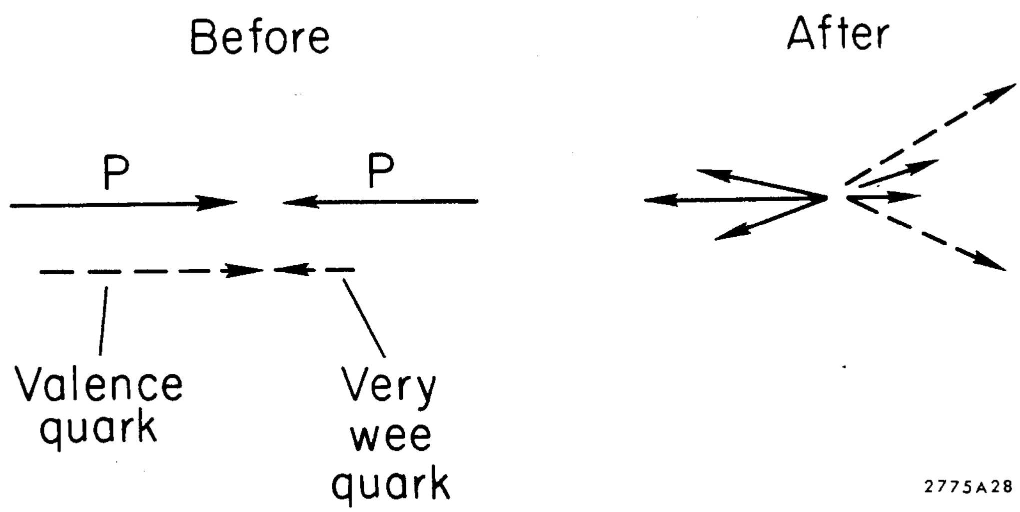

Fig. 27. Configuration of produced jets in CMS frame for q - $\bar{q}$ s-channel annihilation processes. Both jets tend to have comparable rapidities.

However, if the trigger particle is a heavy particle, the opposite-side rapidity distribution peaks at zero rapidity. This is a perplexing situation, which certainly does not favor a dominant $q\bar{q}$ mechanism, and in fact poses problems for any hard collision mechanism.[9]

B. Can Quarks and Antiquarks be the only Relevant Constituents and Fragments?

The answer here is probably no. To study the question, we assume

(i) The factorization hypothesis for quark fragmentation is applicable, i.e., if the process is

$$
pp \rightarrow q + \ldots \quad \longrightarrow \quad \left\{ \begin{array}{l} \pi + \ldots \\ K + \ldots \\ p + \ldots \end{array} \right. \tag{6.4}
$$

the $p_\perp$ distribution of hadron "fragments" depends only on $z = p_\perp$ hadron$/p_\perp$ quark and not on the rest of the environment in the collision (see Eq. (3.2)).

(ii) We also assume that for the relevant $z(\sim 0.7 - 0.9$, Fig. 24) and for a non-strange parent quark

$$
\frac{q \rightarrow K + \ldots}{q \rightarrow \bar{K} + \ldots} \gg 1 \qquad \frac{q \rightarrow P + \ldots}{q \rightarrow \bar{P} + \ldots} \gg 1 \tag{6.5}
$$

Then for a given $p_\perp$ of the jet (or quark)

$$
\frac{pp \rightarrow q + \ldots}{pp \rightarrow \bar{q} + \ldots} \cong \frac{pp \rightarrow K + \ldots}{pp \rightarrow \bar{K} + \ldots} = \frac{pp \rightarrow P + \ldots}{pp \rightarrow \bar{P} + \ldots} \tag{6.6}
$$

Therefore, the ratio of $K/\bar{K}$ to $P/\bar{P}$ should be universal and equal to unity everywhere. Empirically, it is not (Fig. 28).

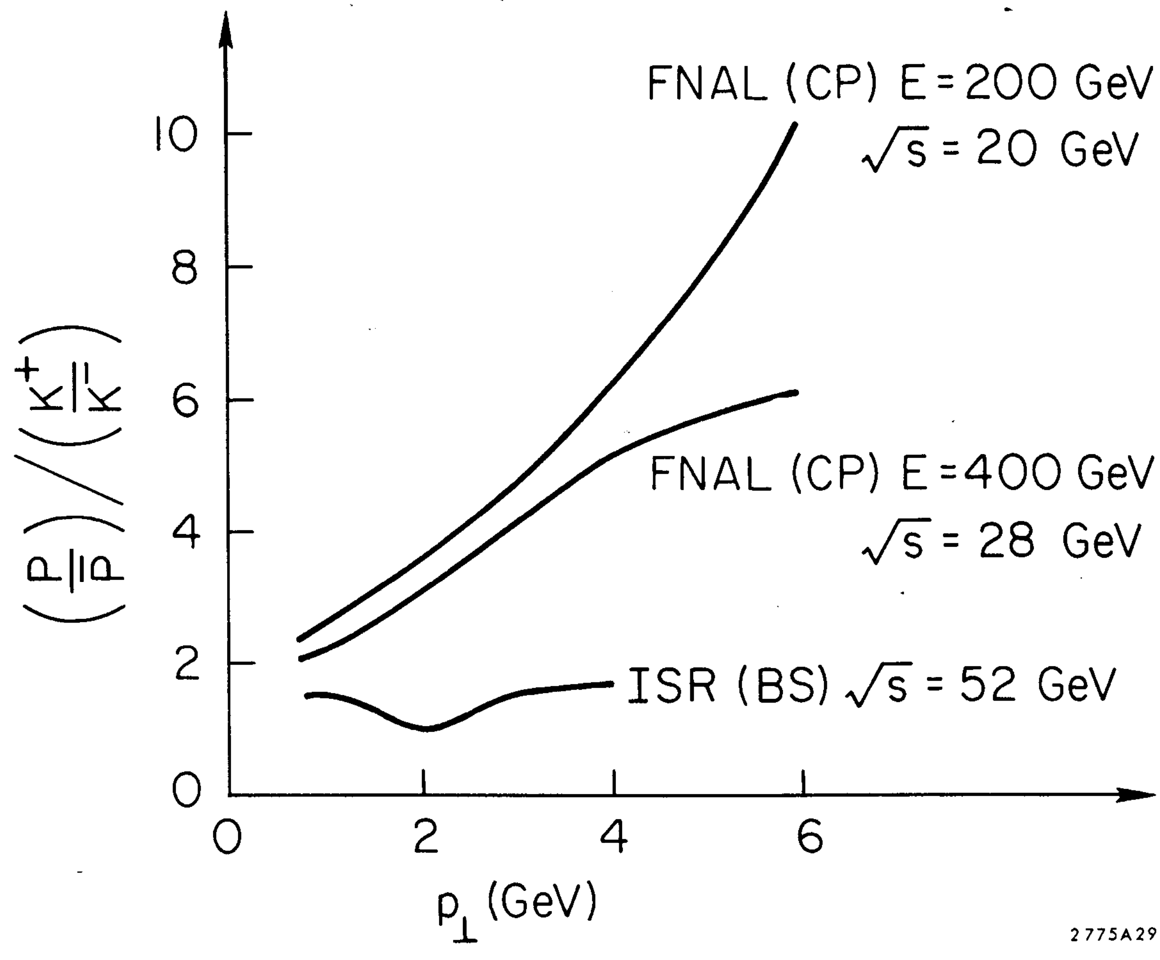

Fig. 28. Ratio of $(p/\bar{p})$ to (K^+/K^-) under various conditions.

C. Conventional Gluons as Partons

According to the parton-model interpretation of deep-inelastic electroproduction data, about 50% of the momentum of an extreme-relativistic proton is not carried by charged constituents. The remainder of the momentum must be carried by neutral constituents, by definition the gluons. What is a gluon?? The simplest notion is that, at least as far as short-distance behavior is concerned, the gluon is a quantum that behaves in a manner similar to the photon. (It can have an internal quantum number such as color, but that will not concern us here.) Then we would be tempted to treat the gluon as another parton like the quark. One then needs to determine its momentum distribution (the analogue to νW_2 for quarks). But there are some constraints on such use of gluons as partons:

(i) Gluons g are valence-partons. However, at large x (such as FNAL energies), the process

$$g + g \to c + d \tag{6.7}$$

must be negligible because this would give a $\overline{P}/P$ and K^-/K^+ ratio of unity, which is very far from the truth. Gluon-quark hard collisions

$$g + q \to g + q \tag{6.8}$$

are not very satisfactory either. The fragments of the gluon cannot provide a high-$p_\perp$ trigger (because such fragments are symmetric in K^+/K^-, etc.). But then the opposite-side jet consists of gluon fragments (which jets empirically look like quark fragments). We arrive at a somewhat contradictory situation, inasmuch as gluon fragments must then provide a trigger as often as the quark fragments.

D. Strings and Bags

We must not forget that the strong interaction which confines quark quantum numbers may turn out to be more exotic than a conventional field-theory description modeled after quantum electrodynamics. If quarks are bound together by strings (flux-tubes of non-abelian gauge field ?), we might entertain the idea of the hard collision as a string-string interaction (Fig. 29). Or if the confinement mechanism involves bags or bubbles (see Sidney Drell's lecture), the hard collision might involve bag fusion followed by fission. However, it is clearly very hard to elevate such thoughts to a level above wild speculations.

E. Diquarks and Triquarks as a Single Constituent

Practitioners of the constituent interchange model have found it of use to consider the diquark, d = (qq), as a single constituent, for example in subprocesses such as

$$q + d \rightarrow B + M \tag{6.9}$$

Likewise, in baryon spectroscopy the diquark is also a useful concept: in non-relativistic SU(6) language, it constitutes the symmetric representation $\underset{\sim}{21}$ contained in $\underset{\sim}{6} \times \underset{\sim}{6}$. Then the baryon B is a bound state of q and d; if the interaction potential is taken to be quark-exchange (interchange??), the spectrum is $\underset{\sim}{6} \times \underset{\sim}{21} = \underset{\sim}{56}$ (L even) + $\underset{\sim}{70}$ (L odd), in good agreement with observation.

Probably the best way of thinking of the diquark is as a positive, short-range correlation in the qq wave-function.

Also of use in the constituent interchange model is the notion of baryons (qqq) or mesons ($q\bar{q}$) as either initial or final constituents which undergo a hard scattering. As a final outgoing constituent, one would naturally identify such an object as a low-mass N* or meson resonance. However, for any process, say

$$a + b \rightarrow B^* + d \tag{6.10}$$

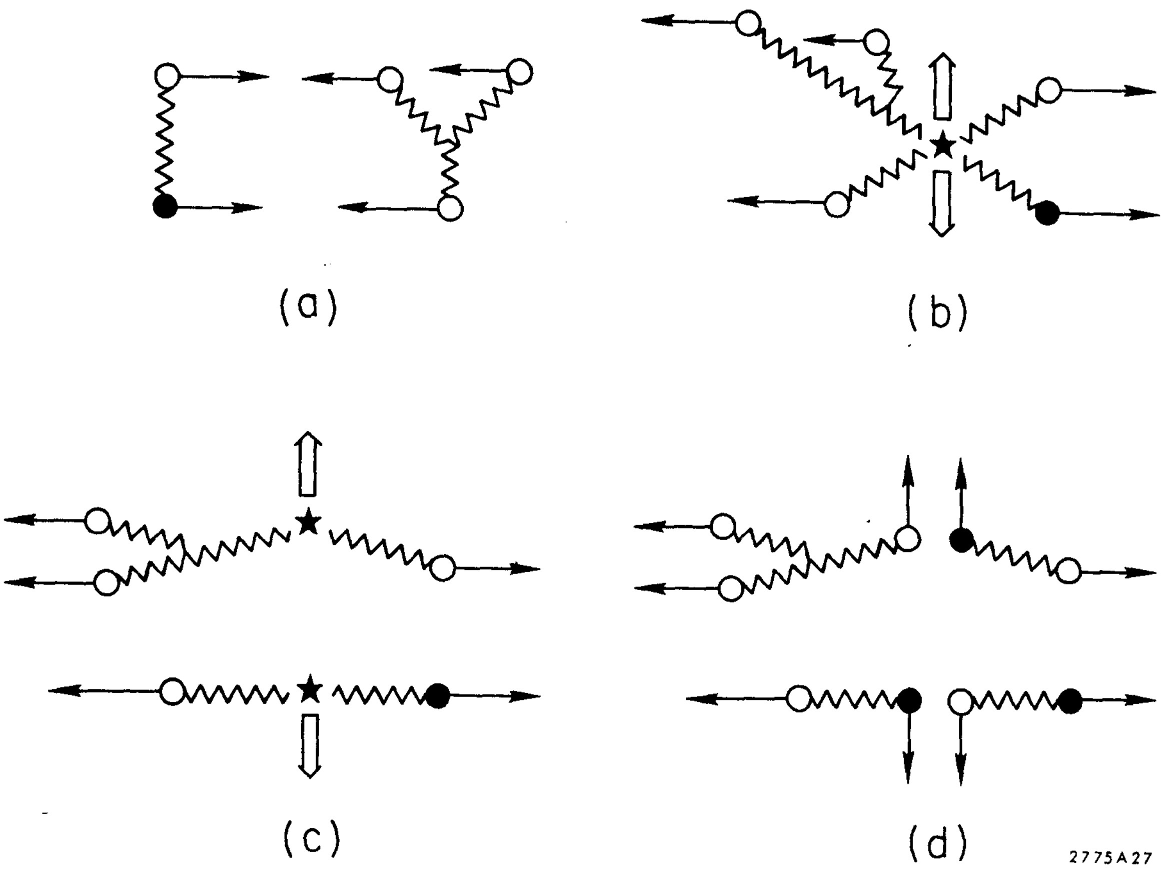

Fig. 29. Possible hard collisions of strings: (a) Before; (b) During. High $p_\perp$ is imparted to string segments at the point of collision. (c) Later; (d) Still later. We have four jets of high $p_\perp$, superimposed in pairs.

it is hard to see why

$$a + b \rightarrow (q + q + q) + d \qquad (6.11)$$

shouldn't also exist, with the q + q + q system a high-mass final state containing a baryon. If the trigger is on the B*, trigger-bias does enhance the importance of the low-mass systems. However, this does not apply to the case where d is the trigger.

As for the role of d, B, M as initial constituents, they may be simply quarks which at the instant of collision have the same impact-parameter and therefore act as a single unit.[10] If this is the case, one might expect a lot of acoplanarity in the final products. For example, the reaction $q + d \rightarrow q + (q + q)$ could lead to a final state with three high-$p_\perp$ jets. There could also be similar mechanisms which are coplanar, e.g., gluodisintegration of the diquark

$$g + d \rightarrow q + q \qquad (6.12)$$

which has its nuclear analogue in photodisintegration of dinucleons in the nucleus.[11]

Another possible mechanism (discussed recently by Landshoff, Polkinghorne, and Scott)[12] is simultaneous scattering of the constituents of a diquark or a baryon (now with arbitrary relative transverse coordinates) from two or three constituents in the other beam. The most characteristic feature of such a mechanism is the existence of not one, but two or three opposite-side high-$p_\perp$ jets, which, however, remain coplanar with the high-$p_\perp$ trigger. If this or the preceding process is in fact relevant, one might well see the effects most prominently at FNAL energies where the interactions of the valence constituents ($x \gtrsim 0.5$) predominate at high $p_\perp$.

F. New Partons or New Hadrons (e.g., Charm)

Let us suppose that the rise in $R = \sigma(e^+e^- \rightarrow \text{hadrons})/\sigma(e^+e^- \rightarrow \mu^+\mu^-)$ at $\sqrt{Q^2} \sim 4$ GeV is at least in part due to pair production of new hadronic partons: $e^+e^- \rightarrow c\bar{c}$. Let us also accept the notion discussed by Harari that the inclusive hadron distribution has two components, as sketched in Fig. 30. This implies that there is very little new component for $x \gtrsim 0.5$ in the inclusive spectrum which, in turn, measures $c \rightarrow$ hadron + ... Therefore, if one makes the very reasonable assumption

$$\frac{pp \rightarrow c + \text{all}}{pp \rightarrow q + \text{all}} \lesssim 1 \tag{6.13}$$

everywhere in phase space, it follows that hadron fragments from $pp \rightarrow c$ + all do not contribute significantly to inclusive spectra at high $p_\perp$.

We must follow such a sweeping assertion with many cautionary words. The first is that the largely untested parton-model assumptions have been used here. The second is that a rare component of "new physics" in the inclusive spectrum in e^+e^- annihilation may be larger at high x than its "old physics" counterpart. The most obvious such candidate is the direct-lepton component.

Also, although the inclusive spectra at high $p_\perp$ is unlikely to be dominated by the products of the new partons, there may be groups of particles produced by "new physics" which do dominate the spectrum of such groups. Thus clever multiparticle triggers utilizing high $p_\perp$ may, in fact, be a very effective way of searching for the new physics in hadron collisions.

We may also discuss the production of new hadrons (let's call them generically D) without reference to any underlying hard collision or parton structure. We begin by guessing the shape of the inclusive spectrum. A decent first try for small $p_\perp$ is

$$E \frac{d\sigma}{d^3p} \overset{?}{\sim} e^{-am_\perp} = e^{-a\sqrt{p_\perp^2 + m^2}} \tag{6.14}$$

This crudely gives a universal behavior for production of π, K, $\bar{p}$, and even J (Fig. 31) with a choice of $a \sim 6\ \text{GeV}^{-1}$. For high $p_\perp$, we might guess $D/\pi \sim$ constant. (This works for K^+/π^+.)

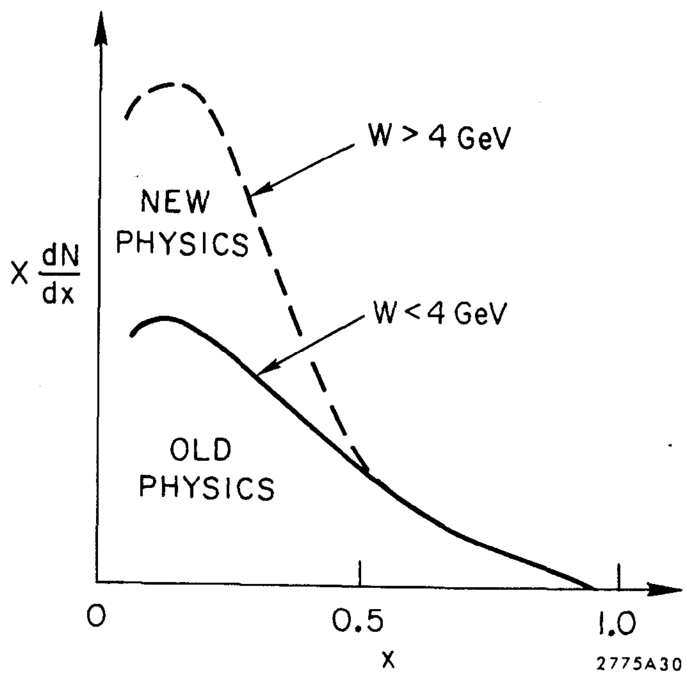

Fig. 30. Conjectured two-component inclusive spectrum for $e^+e^- \rightarrow h$ + anything.

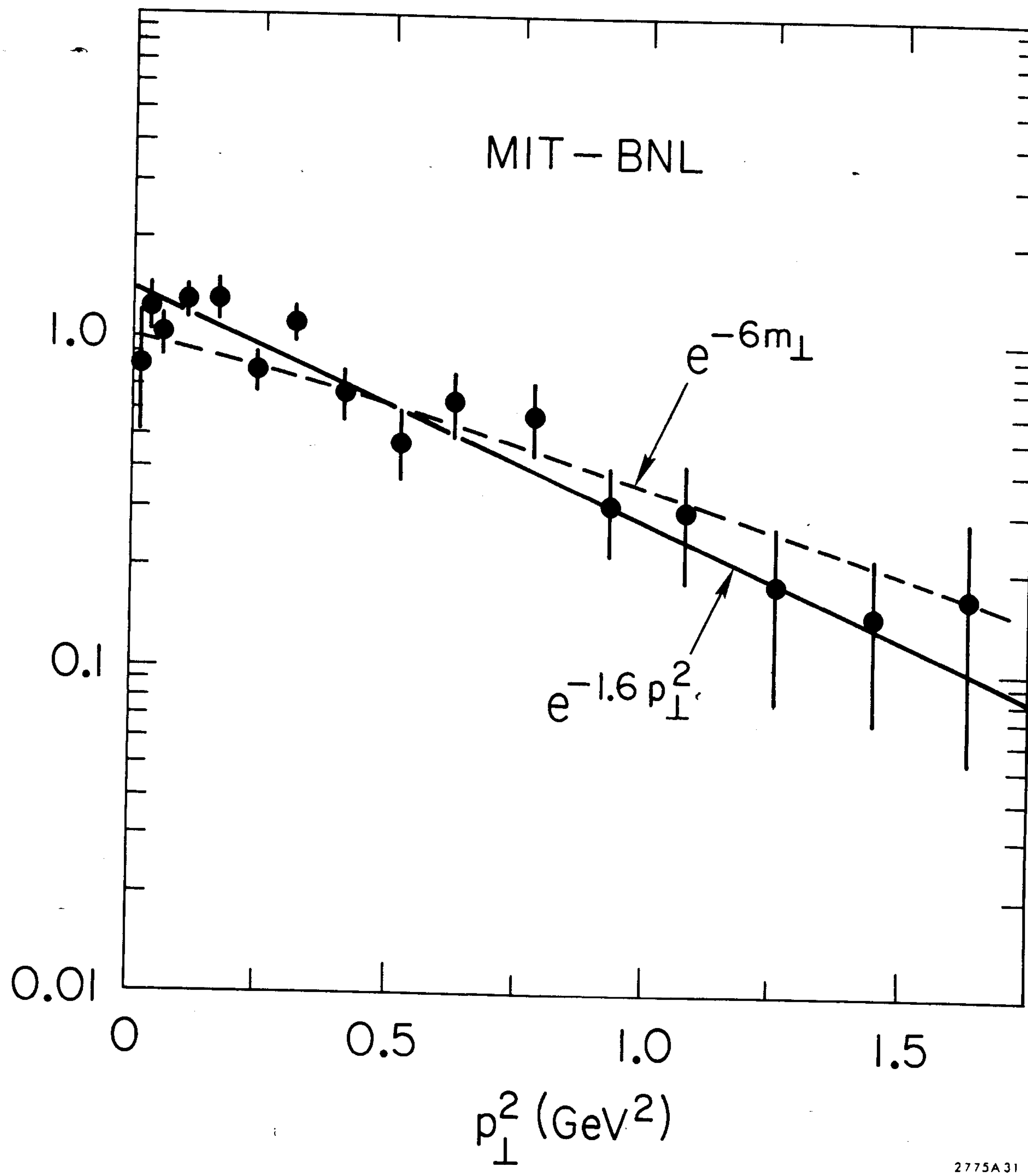

Fig. 31. Transverse-momentum distribution of J as measured by MIT-BNL (cf report of U. Becker to the Topical Conference).

To estimate the size of the inclusive spectrum, we choose production at rest in the cms system at very high energies. Zweig's rule would suggest that D production should exceed ψ production, for which CCRS has measured[13] $d\sigma/dy \sim 10^{-31}$ cm^2. On the other hand, if $D^+/\pi^+ = 1$ at high $p_\perp$, and Eq. (6.14) is used to cut off the low $p_\perp$ yield, one obtains (Fig. 32) a yield $d\sigma/dy$ of D's $\sim 3 \times 10^{-29}$ cm^2. Hence, at ISR energies the guess is

$$3 \times 10^{-29}\ \text{cm}^2 \gg \left.\frac{d\sigma}{dy}\right|_{pp \to D^+ + \ldots} \gg 10^{-31}\ \text{cm}^2 \tag{6.15}$$

Taking $d\sigma/dy \sim 10^{-30}$ cm^2 gives $D^+/\pi^+ \sim 3\%$ at high $p_\perp$. The hadrons from D decay do not contribute to inclusive spectra, as already asserted. Suppose $dN/dx \sim 2(1 - x)$ for a fast hadron emerging from a high-$p_\perp$ decaying D with $x = p_\perp/p_\perp^D$. Then, as in Eq. (5.13),

$$\frac{h}{D^+} = \int_0^1 dx\, x^7 \frac{dN}{dx} \sim 4\% \tag{6.16}$$

giving $h/\pi^+ \sim 10^{-3}$.

Leptons from decaying D's may similarly be estimated. For the 2-body decay, $D^+ \to \ell^+ \nu$, a similar exercise gives

$$\frac{\ell^+}{D^+} \sim \frac{1}{8} B_{D^+ \to \ell^+ \nu} \tag{6.17}$$

or

$$\ell^+/\pi^+ \sim 4 \times 10^{-3} B_{D^+ \to \ell^+ \nu} \tag{6.18}$$

(with an uncertainty of a factor 10). With a 3-body decay, taking very crudely, $dN_\ell/dx \sim 2(1 - x)$ as above, we again get

$$\ell^+/D^+ \sim .04\ B_{D^+ \to \ell^+ M \nu} \tag{6.19}$$

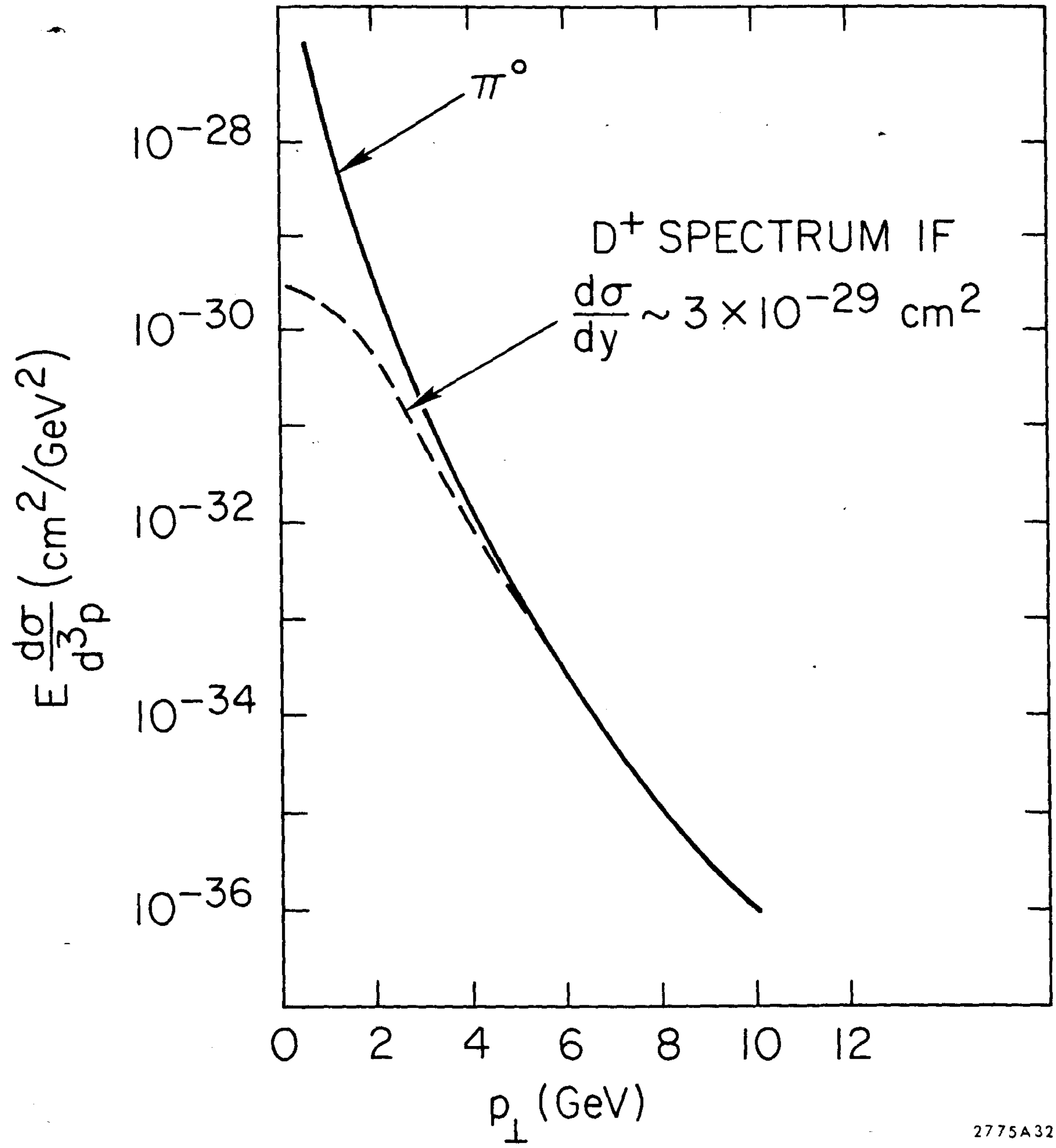

Fig. 32. Conjectured inclusive production of D^{+} at very high energy and $\theta = 90^{o}$. The curve is drawn for a production cross section $\frac{d\sigma}{dy} \sim 30\ \mu b$.

or

$$\ell^+ / \pi^+ \sim 10^{-3} B_{D^+ \to \ell^+ M\nu} \qquad (6.20)$$

again with an uncertainty of a factor 10.

Thus the indications are that, provided the conventional charm-like ideology underlying the new physics is correct, the new physics is probably not a dominant element of high-$p_\perp$ phenomena. However, it is probable that D/π is largest at high $p_\perp$, so that the search for such objects might be easier in that region of phase space. Also, if the "mundane" high-$p_\perp$ phenomena are conclusively shown to be predominantly coplanar, there may be an advantage in studying high-$p_\perp$ non-coplanar events in the search for new particles in hadron-hadron collisions.

VII. CONCLUSIONS and FUTURISM

It should be evident from the previous section that I see no clear picture of the dynamics underlying the hard collision structure. This conservative and gloomy viewpoint is, I expect, not fully shared by the practitioners of the constituent-interchange model, which model by far gives the most comprehensive description of the phenomena.[14] To me, the strongest features of the CIM are its nice accounting of elastic processes, and the smooth connections it makes, via the dimensional-counting rules, to the inclusive processes. In addition, the model has further smooth connections to low-$p_\perp$ physics, i.e., the Regge and resonance physics, as well as incorporating a generalization of duality concepts to high-$p_\perp$ phenomena. And the parton-interchange mechanism is, after all, at the heart of the Feynman picture of low-$p_\perp$ hadron dynamics.

On the negative side, the CIM is not yet a fully quantitative theory. While s and $p_\perp$ dependences are specified, the absolute magnitudes of the individual subprocesses are free parameters. Indeed, with the variety of candidate subprocesses, there are many implicit and explicit free parameters and, to some extent, even functions available. This means there exist many positions of retreat for the model and thereby difficulty in putting the model to a crucial test. While this is not anyone's fault, it still remains a real difficulty in practice. Other possible difficulties rest in understanding correlation data,[9] in particular the large same-side $(\pi\pi)/\pi$ ratio and the opposite-side rapidity correlations found by ACHM and DLR, to which we alluded in Section VIA.

However, the most immediate problem is that hard-collision hypotheses have to be fully established (or disproven). This means in particular

(i) Clarification of the question of coplanarity: are the CERN-SFM and CCR results on $\langle p_N \rangle$ compatible?

(ii) The distribution of the rapidity difference Δy of two opposite-side high-$p_\perp$ particles is needed; it tests whether there is a single opposite-side jet or a more complex distribution, such as fan-shaped.

(iii) The composition of the opposite-side jet components (K/π, p/π, etc.) will be of great value in sorting out various candidates for hard-collision processes. Such data should emerge from two-arm spectrometer measurements at FNAL in the not-too-distant future.

(iv) Scaling behavior of the opposite-side high-$p_\perp$ inclusive distribution (does it depend only on the ratio $p_\perp/p_\perp$ trigger ??) would be of value in testing whether fragmentation-processes for emerging constituents c and d have a universal character.

(v) Measurement of how the inclusive distributions in the beam directions, including identification of particle type, change in the presence of a high-$p_\perp$ trigger would help to reveal the origin of the quantum numbers of the high-$p_\perp$ component.

(vi) Clarification of the properties of lepton-induced jets will be of great use, in particular the check of Feynman scaling for the inclusive spectrum at various Q^2, and the comparison of e^+e^-, e^-, μ^-, and ν-induced jets. Also important is determination of the $\langle p_\perp \rangle$ of leading hadrons ($x > 0.4$) vs Q^2 for e^+e^- jets, as well as eN, μN, and νN deep inelastic processes. The composition of such hadron spectra is also important for comparing with jets in the hadron-hadron collisions.

(vii) Other jet studies in hadron-hadron collisions, using, e.g., calorimeter triggers to study the jet/π^0 ratio, should help remove trigger-bias effects and study more directly the hard collision itself.

(viii) Vital is resolution of the problem of the direct lepton production. The next step, now underway, is looking for dilepton pairs in a large solid-angle experiment, as well as checking the Drell-Yan formula for large-mass dilepton production.

Is all this worth it? I think there is no question; the feasibility and comprehensibility of weak and electromagnetic physics at superhigh-energy pp colliding-beam facilities is almost guaranteed to be good if the lepton jets exist and the Drell-Yan parton-antiparton annihilation mechanism works. And whatever the nature of high-$p_\perp$ hadron reactions, it is background for such physics and must be understood. But beyond such mundane considerations lies the promise that the high-$p_\perp$ hadron dynamics gets at fundamentals of strong interactions. If so, while it will be a long and difficult task to understand the phenomenon, it will be well worth the effort.

References

1. SBB, as cited in Section I.
2. F. Büsser et al., Phys. Letters 51B, 306 (1974).
3. See, for example, J. Bjorken, Proceedings of the SLAC Summer Institute on Particle Physics, 1973, Vol. 1, ed. M. Zipf.
4. Taken from the reviews of M. Perl and B. Richter; Proceedings of the XVII International Conference on High Energy Physics, London (1974).
5. R. Huson, invited talk at the Spring Meeting of the American Physical Society, Washington, D. C. (1975).
6. J. Dakin et al., Phys. Rev. D10, 1401 (1975).
7. D. Caldwell et al., "Searching for Quarks with Photons," paper submitted to Palermo Conference (unpublished).
8. See, for example, B. Combridge, Phys. Rev. D10, 3849 (1974).
9. This is studied in detail, in the context of the constituent interchange model, by R. Raitio and G. Ringland, preprint SLAC-PUB-1620.
10. This idea was introduced to me via E. Levin and L. Frankfurt (private communication).
11. J. Levinger, Phys. Rev. 84, 43 (1951).
12. P. Landshoff, J. Polkinghorne, and D. Scott, preprint DAMPT 75/13.
13. R. Cool, these Proceedings.
14. A good review of CIM is contained in SBB (Ref. 1).